

General Disclaimer

One or more of the Following Statements may affect this Document

- This document has been reproduced from the best copy furnished by the organizational source. It is being released in the interest of making available as much information as possible.
- This document may contain data, which exceeds the sheet parameters. It was furnished in this condition by the organizational source and is the best copy available.
- This document may contain tone-on-tone or color graphs, charts and/or pictures, which have been reproduced in black and white.
- This document is paginated as submitted by the original source.
- Portions of this document are not fully legible due to the historical nature of some of the material. However, it is the best reproduction available from the original submission.



**NASA CR-167868
IITRI-M06071-20**

CREEP OF PLASMA SPRAYED ZIRCONIA

(NASA-CR-167868) CREEP OF PLASMA SPRAYED
ZIRCONIA Final Report (IIT Research Inst.)
61 p HC A04/MF A01 CSCL 11B

N83-29393

**Unclas
G3/27 28288**

**R.F. FIRESTONE, W.R. LOGAN AND J.W. ADAMS
IIT RESEARCH INSTITUTE
10 WEST 35TH STREET
CHICAGO, ILLINOIS 60616**

NOVEMBER 1982

**PREPARED FOR
NATIONAL AERONAUTICS AND SPACE ADMINISTRATION
LEWIS RESEARCH CENTER, CLEVELAND, OHIO**

CONTRACT NOS. NAS 3-20828 AND NAS 3-22127

1. Report No. CR 167868	2. Government Accession No.	3. Recipient's Catalog No.	
4. Title and Subtitle Creep of Plasma Sprayed Zirconia		5. Report Date Nov. 1982	
		6. Performing Organization Code	
7. Author(s) R. F. Firestone, W. R. Logan, J.W. Adams		8. Performing Organization Report No. IITRI-M06071-20	
		10. Work Unit No.	
9. Performing Organization Name and Address IIT Research Institute 10 W. 35th Street Chicago, IL 60616		11. Contract or Grant No. NAS 3-20828 NAS 3-22127	
		13. Type of Report and Period Covered Final	
12. Sponsoring Agency Name and Address National Aeronautics and Space Administration Washington, DC 20456		14. Sponsoring Agency Code	
		15. Supplementary Notes Project Manager: Robert C. Bill NASA-Lewis Research Center Cleveland, Ohio	
16. Abstract Specimens of plasma-sprayed zirconia thermal barrier coatings with three different porosities and different initial particle sizes were deformed in compression at initial loads of 1000, 2000, and 3500 psi and temperatures of 1100°, 1250°, and 1400°C. The coatings were stabilized with lime, magnesia, and two different concentrations of yttria. Creep began as soon as the load was applied and continued at a constantly decreasing rate until the load was removed. Temperature and stabilization had a pronounced effect on creep rate. The creep rate for 20% Y ₂ O ₃ -80% ZrO ₂ was 1/3 to 1/2 that of 8% Y ₂ O ₃ -92% ZrO ₂ . Both magnesia and calcia stabilized ZrO ₂ crept at a rate 5 to 10 times that of the 20% Y ₂ O ₃ material. A near proportionality between creep rate and applied stress was observed. The rate controlling process appeared to be thermally activated, with an activation energy of approximately 100 cal/gm mole °k. Creep deformation was due to cracking and particle sliding.			
ORIGINAL PAGE IS OF POOR QUALITY			
17. Key Words (Suggested by Author(s)) Ceramic Abradable Steel Zirconia Thermal Barrier Plasma-sprayed Creep High Temperature		18. Distribution Statement UNLIMITED	
19. Security Classif. (of this report) Unclassified	20. Security Classif. (of this page) Unclassified	21. No. of Pages 58	22. Price*

* For sale by the National Technical Information Service, Springfield, Virginia 22161

ORIGINAL PAGE IS
OF POOR QUALITY

FOREWORD

We wish to acknowledge the assistance of Dr. Thomas A. Taylor of the Linde Division of Union Carbide Corporation for his development of the technique for specimen preparation. We also wish to thank the NASA-Lewis Project Manager, Dr. Robert C. Bill, for his patience and support of the program.

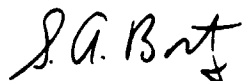
Respectfully submitted,

IIT RESEARCH INSTITUTE



Ross F. Firestone
Senior Scientist

Approved:



S. A. Bortz, Manager
Nonmetallic Materials and Composites
Materials Technology

IIT RESEARCH INSTITUTE

ABSTRACT

Specimens of plasma-sprayed zirconia thermal barrier coatings with three different porosities and different initial particle sizes were deformed in compression at constant loads with initial stresses of 1000, 2000, or 3500 psi and temperatures of 1100°, 1250°, or 1400°C. The coatings were stabilized with calcia, magnesia, or two different concentrations of yttria. Creep began as soon as the load was applied and continued at a constantly decreasing rate until the load was removed. Temperature and stabilization had a pronounced effect on creep rate. The creep rate for 20% Y_2O_3 -80% ZrO_2 was 1/3 to 1/2 that of 8% Y_2O_3 -92% ZrO_2 . Both magnesia and calcia stabilized ZrO_2 crept at a rate 5 to 10 times that of the 20% Y_2O_3 material. A near proportionality between creep rate and applied stress was observed. The rate controlling process appeared to be thermally activated, with an activation energy of approximately 100 cal/gm mole °K. Creep deformation was due to cracking and particle sliding.

TABLE OF CONTENTS

	<u>Page</u>
1. INTRODUCTION.	1
1.2 Task Summary	2
2. BACKGROUND.	3
2.1 Plasma Spray Deposition of Ceramic Coatings.	3
2.2 Creep Testing of Thermal Barrier Coatings.	4
2.3 Experimental Procedure	5
2.4 Creep Deformation.	17
3. CONCLUSION.	29
REFERENCES.	30
APPENDIX.	31

LIST OF TABLES

<u>Table</u>	<u>Page</u>
1 Plasma Spray Powders.	7

LIST OF FIGURES

<u>Figure</u>	<u>Page</u>
1 Free standing ZrO_2 cylinder sample.	6
2 Cerac 20% yttria, 80% zirconia powder	8
3 Metco 20% yttria, 80% zirconia powder	8
4 Cerac 8% yttria, 92% zirconia powder.	9
5 Metco 31% lime, 69% zirconia powder	9
6 Plasmadyne 21% magnesia, 79% zirconia powder.	10
7 System ZrO_2 - Y_2O_3	10
8 System ZrO_2 -CaO, tentative, at high temperature	11
9 System ZrO_2 -MgO showing ZrO_2 -rich side.	11
10 Plasma-sprayed Y_2O_3 - ZrO_2 on aluminum mandrel.	13
11 Overall view of creep furnace with door open, showing load system.	14
12 Schematic of load train and extensometer of creep apparatus . . .	15
13 Specimen in creep apparatus	16
14 Typical creep curves.	19
15 Effect of porosity on creep deformation	20
16 Effect of temperature and stress on creep deformation	21
17 Effect of particle size on creep deformation.	22
18 Effect of varying yttria content on creep deformation	24
19 Effect of different stabilizers on creep deformation.	25
20 Cross section of specimen wall showing layered particles.	26
21 Outer surface of magnesia-stabilized zirconia uncrept specimen. .	26
22 Outer surface of magnesia-stabilized zirconia specimen after 5% creep deformation.	28

1. INTRODUCTION

The efficiency of a gas turbine engine is sensitive to operating clearances over the blade tips throughout the engine. The single location where clearances have the greatest impact on efficiency is in the high pressure turbine. Here 0.5% to 1% increase in SFC is suffered for each 1% increase in clearance-to-blade span ratio. Use of abradable ceramic seal materials over the high pressure turbine blade tips allows the high pressure turbine to operate at minimum clearances, and reduce, the cooling air demand required for conventional metallic seal materials. Increased turbine operating temperatures are putting increased importance on the application of abradable ceramic materials to replace the metallic systems.

Plasma-spray-deposited yttria-stabilized zirconia coatings are excellent for this application. However, because they are brittle, cracks may develop which can cause failure. By placing the coating under compression, failure can be prevented since cracks cannot propagate in a compressive stress field. To be effective, the compressive stress must be maintained within a controlled range throughout the entire range of operating temperatures.

Ceramics placed under stress at high temperatures tend to deform to relieve the stress so that the creep behavior of these coatings is important. Previous work on conventional yttria-stabilized zirconia ceramics has shown excellent resistance to creep. There have been no studies on plasma-spray-deposited coatings which, because of the method of forming, may behave differently. Thus, a determination of the creep rates and an understanding of the mechanisms of creep deformation is essential for the application and improvement of plasma-spray-deposited yttria-stabilized zirconia coatings.

1.1 PROGRAM OBJECTIVES

The objectives of this program were: to determine the creep behavior of plasma-sprayed-deposited yttria-stabilized zirconia and to elucidate the underlying mechanisms. This was achieved by preparing well-characterized coatings, carefully measuring their creep deformation, and analyzing the specimens and creep behavior.

1.2 TASK SUMMARY

The program was conducted in four tasks: specimen preparation, creep deformation, identification of creep mechanisms, and reporting progress and results.

Specimen preparation was carried out by Union Carbide Coating Service, Indianapolis, Indiana, using automated production equipment, and at IIT Research Institute using laboratory equipment.

Creep deformation was performed at constant compressive load in air at various initial stresses and temperatures. The deformation rate was recorded continuously. The effect of changes in temperature, stress, porosity, microstructure, and chemical composition on the high-temperature creep deformation was determined. Since this was a preliminary investigation, a wide range of parameters were investigated and only a few specimens were subjected to creep at each condition.

Identification of creep mechanisms was carried out by analysis of data from creep tests and isothermal annealing, and by microscopic examination of specimens before and after creep or annealing.

Monthly letter progress reports were made during the program.

2. BACKGROUND

2.1 PLASMA SPRAY DEPOSITION OF CERAMIC COATINGS

Coatings may be deposited by plasma spraying of any ceramic material which melts to form a liquid with a reasonably low vapor pressure. In the plasma spray process, ceramic powder is entrained in a carrier gas, passed through an arc-generated plasma which melts the powder, and propelled as a molten droplet onto the part to be coated where it is rapidly solidified. A strong bond can form at the interface between the part and the coating. The coated part may be subjected to a post-spray treatment to change the properties of the coating and interface.

Plasma-spray-deposited coatings have high internal energy which arises from the rapid cooling and solidification inherent in the process. Since the material is quenched from a liquid phase, any phase which is in equilibrium for a given composition from liquidus to room temperature may be present in the coating depending on kinetics and cooling rate. These metastable phases may have a strong effect on the properties of the coating. In addition, the quench also introduces residual stresses which can be locally intense if the coating material has anisotropic thermal contraction. Heating the coating may cause phase changes to occur, relaxation of residual stresses, and significant changes in the properties of the coating.

The forming conditions for plasma-spray-deposited coatings make them quite different from conventional ceramics. Conventional ceramics are heated and cooled slowly and usually soaked at the firing temperature which is usually much lower than the melting temperature for a long time so they are likely to be nearly in equilibrium; and, if the cooling rate is slow, the equilibrium temperature of the ceramic may be close to room temperature. Thus, the internal energy of conventional ceramics may be quite low by comparison and heating then produces fewer changes.

Creep is the plastic deformation of a material by a long-term stress. The parameters involved in a creep experiment with constant load or constant stress are: stress (σ), temperature (T), and time (t). The creep deformation

can be characterized by the plastic strain (ϵ) and the strain rate ($\dot{\epsilon} = d\epsilon/dt$). Creep is conventionally divided into three parts: 1) Primary or transient creep (ϵ_t) with a constantly decreasing creep rate; 2) secondary or steady-state creep (ϵ_s) with a constant (minimum) creep rate ($\dot{\epsilon}_s$); and 3) tertiary creep (ϵ_{tt}) with an increasing creep rate which terminates in failure of the specimen. In addition, there is an initial strain on loading (ϵ_0) which is composed of elastic deformation which occurs during loading. The absolute and relative extent of the three stages can vary greatly depending on the material and experimental parameters. The third stage is often absent in compressive creep.

All of the theoretical creep models presently available were developed on the basis of a fully dense material. However, plasma-sprayed ceramic coatings contain porosity. It is generally observed that creep increases with increasing porosity. The one comprehensive study was made on alumina¹ in which pores were produced by introduction of naphthalene during forming which "burned out" during firing. Grain boundary sliding was the principal mechanism of creep strain observed.

There have been four recent papers on compressive creep of yttria-stabilized zirconia formed by conventional ceramic techniques.²⁻⁵ The studies concentrated on steady-state creep since primary creep was variable and tertiary creep was not reached.

The general conclusions were that yttria-stabilized zirconia has a low creep rate which is strongly dependent on microstructure but not on purity of the material. The mechanism of grain boundary sliding for fine grain material at low stresses seems to be well established, but there is no direct evidence for the dislocation models which have been proposed.

2.2 CREEP TESTING OF THERMAL BARRIER COATINGS

In a creep test a specimen is heated to a constant temperature and a load is applied. The specimen deforms under the load and the deformation is measured as a function of time. The temperature must be closely controlled since the specimen will expand or contract if the temperature changes.

A constant load can be used on the specimen for simplicity. While it is possible to use mechanical or electrical devices to maintain constant stress

on the specimen, this requires assumptions of deformation behavior for calibration.

Since plasma-spray-deposited coatings are quite thin and the load is to be applied in the plane of the coating, the specimen geometry and method of loading are important.

A coating may be tested either in situ on the substrate or removed from the substrate and tested alone. The coated substrate makes a more robust specimen which is easier to handle. If the creep behavior of the substrate is known, the creep behavior of the coating may be obtained by making certain assumptions about the interface. However, the substrate is subject to oxidation at the temperatures of interest which introduces some uncertainty in the tests. Hence, a free-standing coating specimen was selected.

Testing a specimen of a coating without the substrate is difficult since it is very fragile, especially if the coating is of normal thickness. The coating may be built up to greater thickness but this coating may not be representative. Consequently, a coating of normal thickness was selected.

After careful considerations and calculations, a compressively loaded specimen in the form of a hollow cylinder was decided upon (Figure 1). With a coating of normal thickness, about 0.030 in., a cylinder of 0.25 in. I.D. by 0.5 in. long will sustain the specified stresses without buckling up to at least 10% strain and be reasonably free of end effects.

2.3 EXPERIMENTAL PROCEDURE

Hollow cylindrical specimens were prepared by plasma spraying and deformed in air under constant compressive loads of 1000, 2000, or 3500 psi initial stress at temperatures of 1100°C (2010°F), 1250°C (2280°F), or 1400°C (2560°F). Three apparent porosities were studied: 11, 13, and 15%.

ORIGINAL PAGE IS
OF POOR QUALITY

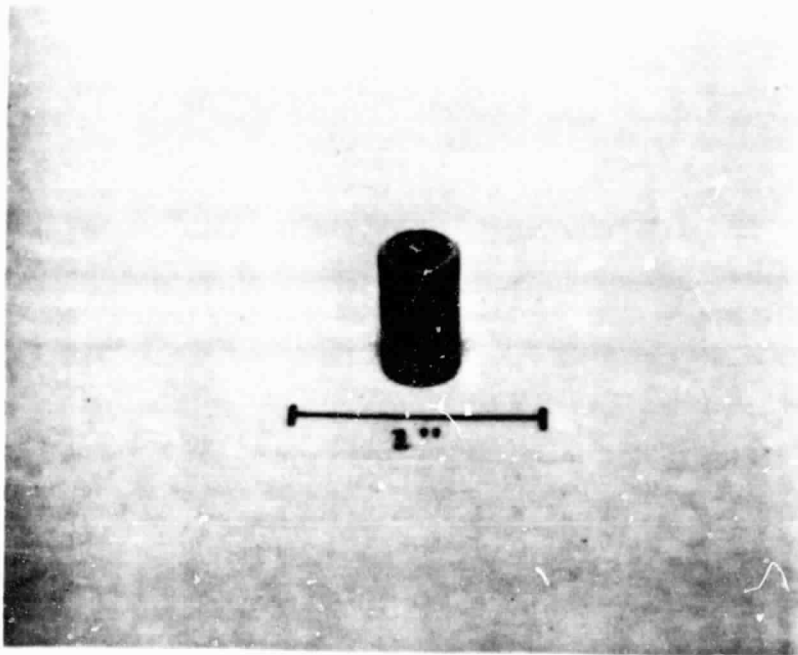


Figure 1. Free standing ZrO_2 cylinder sample.

TABLE 1. PLASMA SPRAY POWDERS

<u>Composition, wt%</u>	<u>Powder Source</u>	<u>Particle Size, microns</u>
20 Yttria, 80 Zirconia	Cerac	-44
20 Yttria, 80 Zirconia	Metco	-88 +10
8 Yttria, 92 Zirconia	Cerac	-74 +44
31 Lime, 69 Zirconia	Metco 211	-53 +10
21 Magnesia, 79 Zirconia	Plasmadyne 359-F	-88 +10

The ceramic powders used for specimen preparation were obtained from commercial sources and are listed in Table 1. SEM photomicrographs were taken of each powder to determine particle size and morphology. Of the two 20% yttria-80% zirconia powders, the Cerac (Fig. 2) was the finer and was composed of discrete particles, while the Metco powder (Fig. 3) was composed of large spray-dried agglomerates with a finer ultimate particle size. The Cerac 8% yttria-92% zirconia powder (Fig. 4) and the Plasmadyne magnesia-stabilized zirconia powder (Fig. 5) were also agglomerates but not spray-dried, while the Metco lime-stabilized zirconia powder (Fig. 6) was composed of discrete particles.

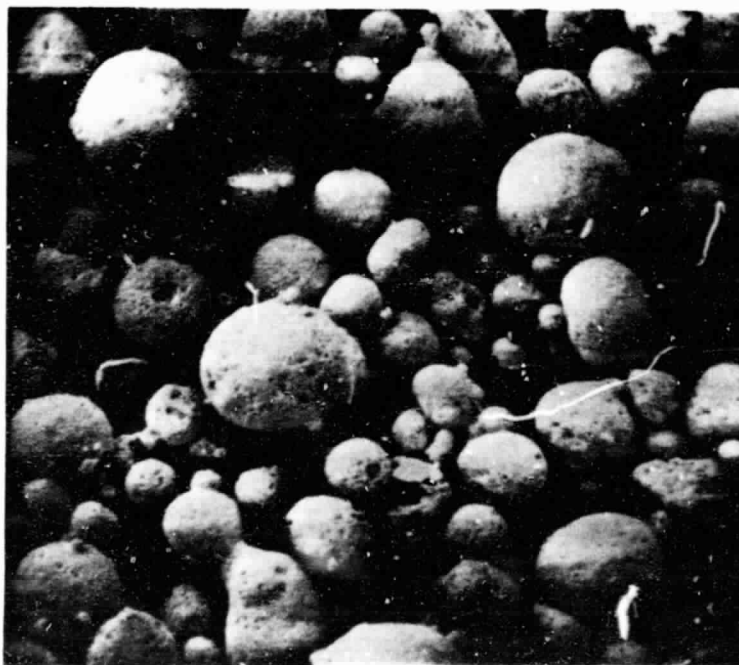
Although all powder compositions are supposed to fully stabilize zirconia in the cubic phase, there is a large difference in their phase diagrams. Yttria at either 8 or 20 wt% forms a solid solution which stabilizes the cubic phase of zirconia down to at least 1000°C (Fig. 7). Lime at 31 wt% also produces stable cubic zirconia down to at least 1400°C (Fig. 8). However, magnesia at 21 wt% produces stability down to approximately 1800°C where there is a separation of a tetragonal zirconia solid solution from the cubic solid solution, and at 1400°C the cubic solid solution disappears (Fig. 9). Of course, because of the sluggishness of solid state reactions, these changes may not occur during the rapid cooling following spraying.

ORIGINAL PAGE IS
OF POOR QUALITY



200X

Figure 2. Cerac 20% yttria, 80% zirconia powder.



200X

Figure 3. Metco 20% yttria, 80% zirconia powder.

ORIGINAL PAGE IS
OF POOR QUALITY



200X

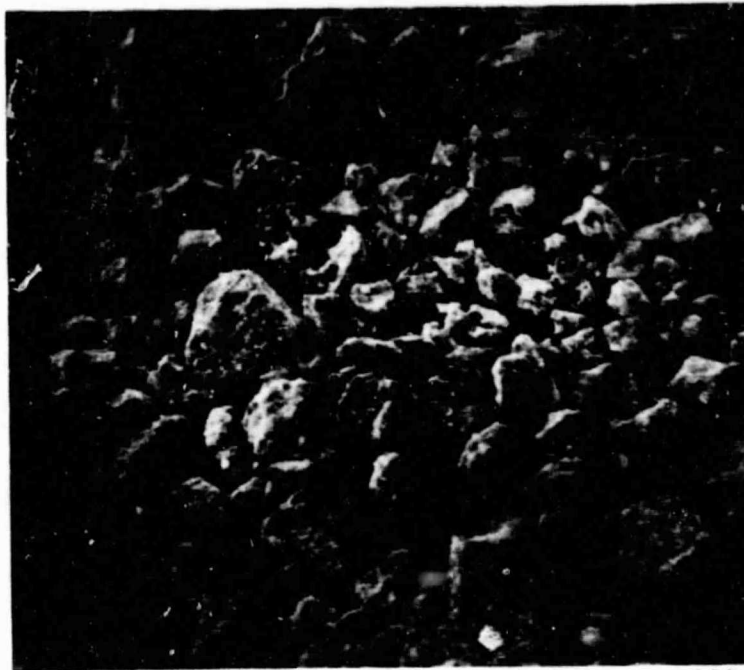
Figure 4. Cerac 8% yttria, 92% zirconia powder.



200X

Figure 5. Metco 31% lime, 69% zirconia powder.

ORIGINAL PAGE IS
OF POOR QUALITY



200X

Figure 6. Plasmadyne 21% magnesia,
79% zirconia powder.

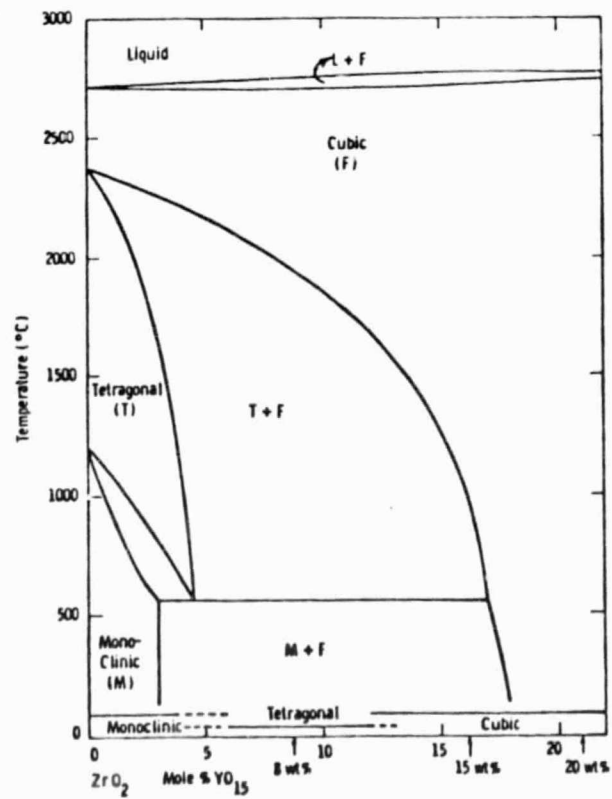


Figure 7. System ZrO_2 - Y_2O_3 .

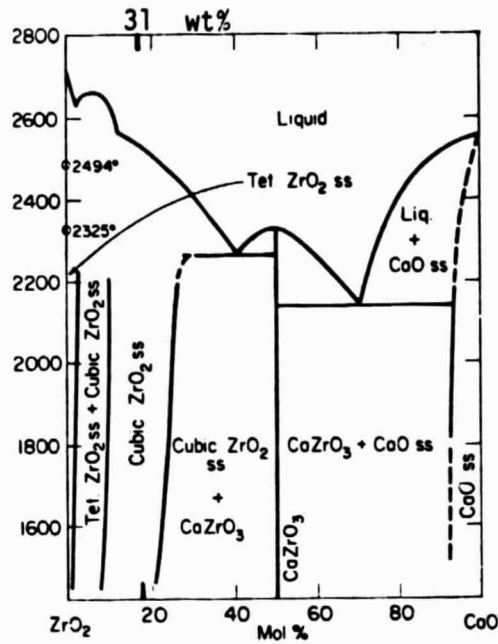


Figure 8. System ZrO_2 - CaO , tentative, at high temperature. High-temperature phase relations in the ZrO_2 -rich region are uncertain.⁷

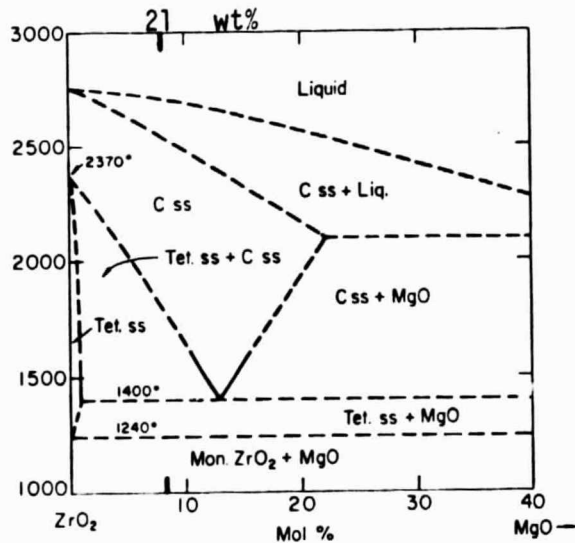


Figure 9. System ZrO_2 - MgO showing ZrO_2 -rich side.⁸

The first specimens were prepared by Union Carbide^a who developed the technique of producing them. Ceramic powder was plasma-sprayed onto a hollow aluminum mandrel until a 1/32 in. thick coating was produced (Figure 10). The center of the mandrel was bored out until only a few thousandths of an inch of metal was left. The residual metal was removed by solution in sodium hydroxide followed by washing and drying in water. After fabrication, specimen dimensions were measured and porosity was determined. Complete details on specimen preparation are given in the appendix.

Specimens were deformed in air with a constant compressive load under isothermal conditions. The creep apparatus is shown in Fig. 11 and schematically in Fig. 12. A load lever, pivoted at one end, was loaded at the other by a funnel containing lead shot. The lever transferred the load through a stainless steel and SiC load rod to an alumina platen which rested on the specimen. Specimen reaction was transferred through another alumina platen, then through a SiC and stainless steel load rod, to a load cell which measured the applied load. The load train was aligned by the stainless steel load rods which passed through precision water-cooled bushings above and below the specimen. The alumina platens were coaxial and aligned plane and parallel within 0.001 in. per in.

Specimen deformation was measured with a DCDT transducer which was connected to 1/8 in. diameter alumina push rods which bore on the top and bottom platens (Fig. 13). This differential extensometer compensated for any temperature differences along the rods and was independent of the load train. Accuracy was within 0.1% strain.

The specimens were heated in a silicon carbide element resistance furnace whose temperature was proportionally controlled with a platinum/rhodium thermocouple adjacent to the elements. Specimen temperature was measured with a similar thermocouple cemented to the bottom platen. Initial calibration of test temperatures was made by cementing a thermocouple to a dummy specimen. Accuracy of temperature measurement was $\pm 1^{\circ}\text{C}$ (2°F); accuracy of temperature control was $\pm 2^{\circ}\text{C}$ (4°F).

^aLinde Division, Union Carbide Corporation, Indianapolis, Indiana.

ORIGINAL PAGE IS
OF POOR QUALITY

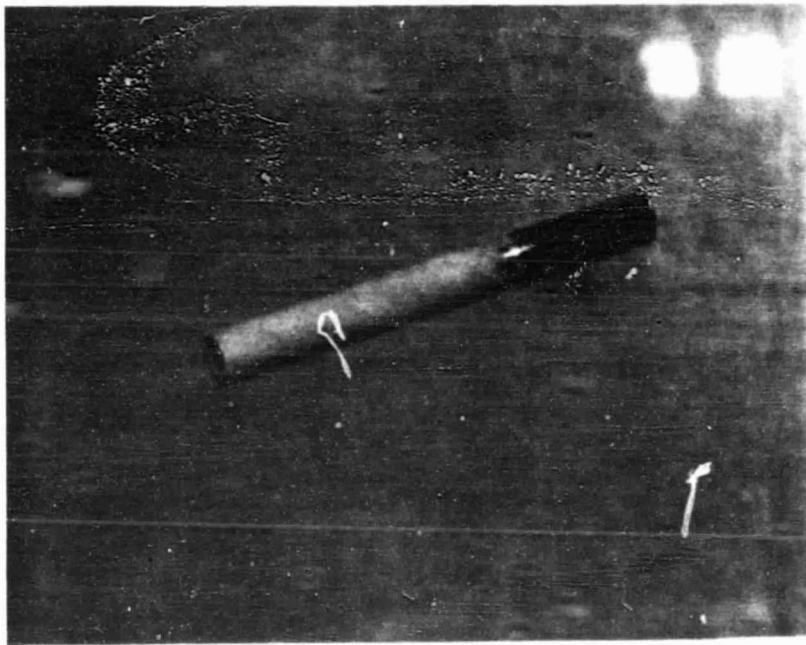


Figure 10. Plasma-sprayed $Y_2O_3-ZrO_2$ on aluminum mandrel.

ORIGINAL PAGE IS
OF POOR QUALITY

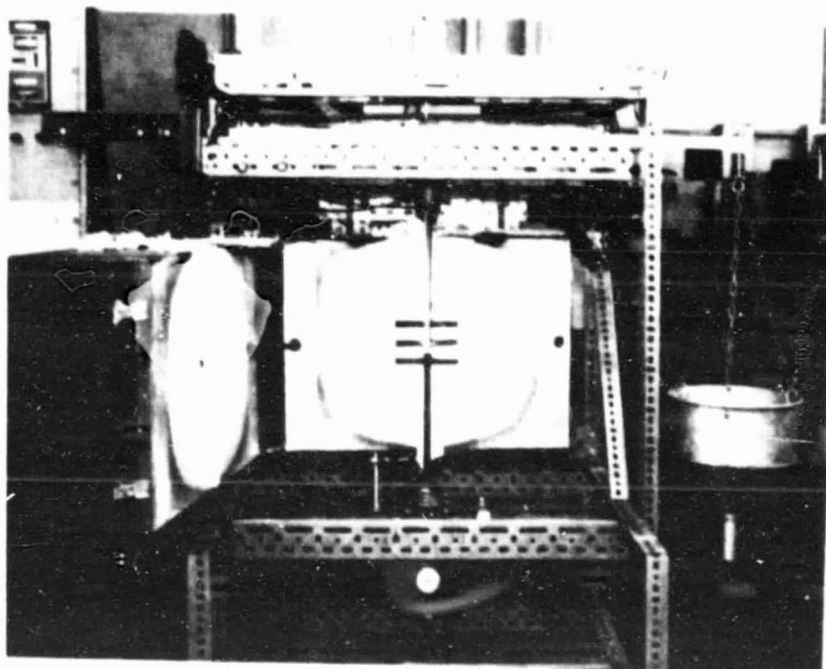


Figure 11. Overall view of creep furnace with door open, showing load system.

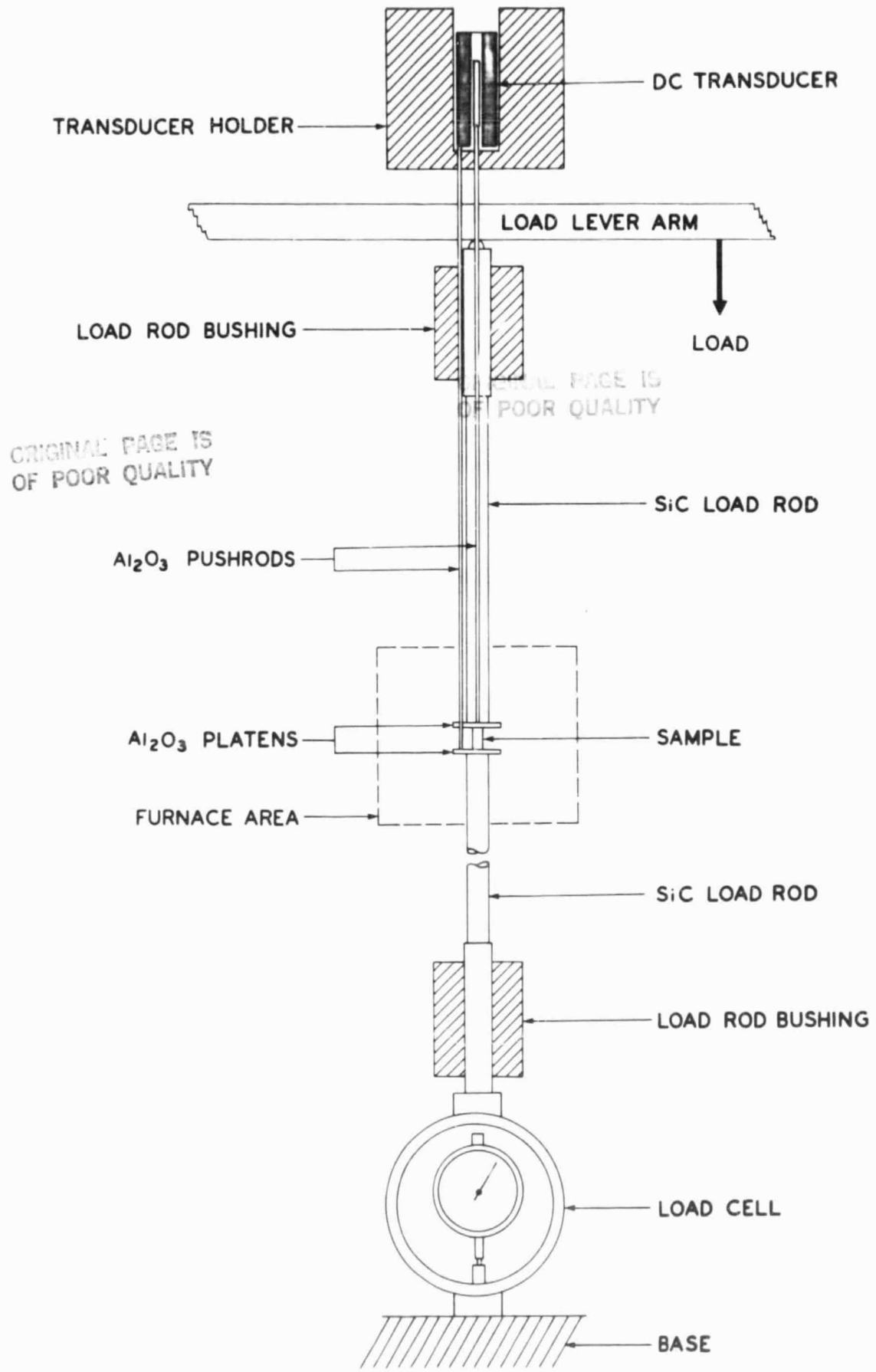


Figure 12. Schematic of load train and extensometer of creep apparatus.

ORIGINAL PAGE IS
OF POOR QUALITY

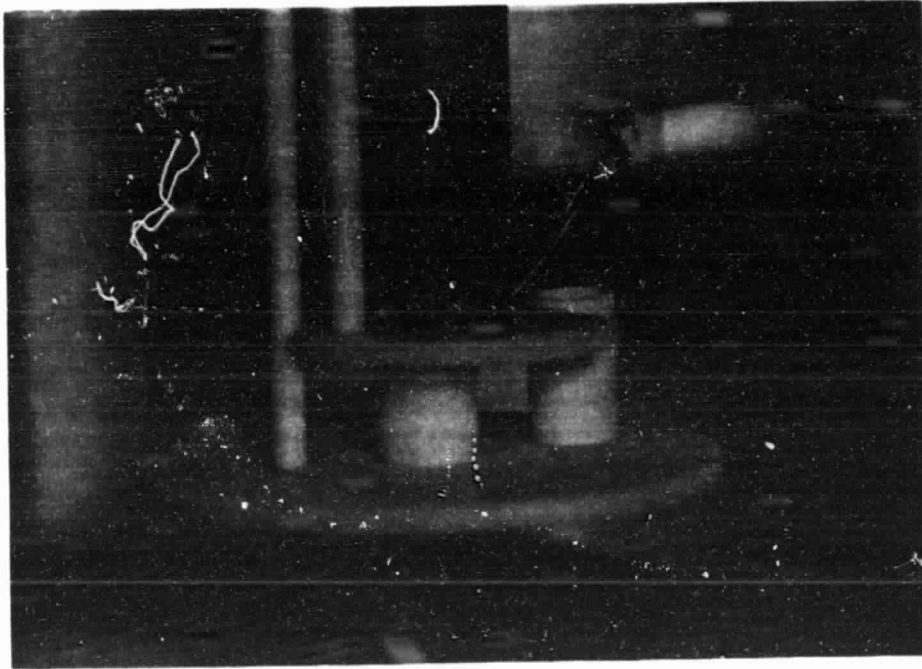


Figure 13. Specimen in creep apparatus.

To determine if any of the deformation was due to sintering shrinkage, an identical but unloaded specimen was placed on the lower platen next to the loaded specimen (see Fig. 13). In all cases, the shrinkage was less than 0.1%.

Specimen temperature and deformation were recorded continuously during creep deformation. After deformation, specimen dimensions and porosity were measured. Specimen microstructures before and after creep were studied using optical microscopy and SEM.

A creep test was begun by carefully aligning the specimen in the test apparatus and applying a small load to maintain alignment. The furnace was then heated to the desired temperature at the rate of 500°C/hr (900°F/hr). After a 2 hr stabilization at temperature, lead shot was slowly poured into the load funnel until the load cell indicated the desired load. When 5% engineering strain or 250 hr time had elapsed, the test was terminated. The specimen was cooled in the furnace to room temperature under load to preserve the creep microstructure.

2.4 CREEP DEFORMATION

Creep began as soon as the load was applied and continued at a decreasing rate until the test was ended. Steady-state creep was never reached. The initial part of the creep curve showed wide variation, but after 1% strain the creep strain, ϵ , could be related to the time, t , by the equation:

$$\epsilon = e^{Bt^{1/2}}$$

where $-2 \leq B \leq +2$. Hence, on a log-log plot, the creep curves appear, for the most part, as straight lines.

Because the ends of the specimen were constrained by the platens, slight barrelling of the specimen occurred during creep. This was minimized by limiting creep strain to 5% or less. For strains greater than 15%, the specimen buckled, and at 22% strain, sinusoidal buckling was observed (Fig. 13).

Porosity was the first parameter investigated. Specimens were prepared by Union Carbide from Cerac 20% yttria-80% zirconia powder with three different porosities: 13%, which was designated baseline porosity since it was

typical of normal commercial practice; 11%, which was the lowest that could be obtained without post-spraying heat treatment; and 15%, which was the highest that could be obtained without adding fugitive powders and still yield a sound coating. Creep deformation versus time curves for these three different porosities are shown in Fig. 14. They are typical of the deformation of all the other materials studied. When the logarithm of deformation is graphed versus the logarithm of time, the curves are straight lines of nearly constant slope (Fig. 15). These results showed that variations in porosity within normal limits had very little effect on the creep deformation rate. All subsequent specimens were sprayed to baseline porosity.

The effect of changes in the temperature and stress are shown in Fig. 16 for two stresses--2000 and 3500 psi--and three temperatures--1100°, 1250°, and 1400°C. The pronounced effect of temperature and lesser effect of stress are clearly shown. Calculations using an Arrhenius equation for a singly activated process over the temperature range of the experiments gives an effective activation energy of approximately 100 cal/gm-mole °K. However, this value cannot be used to identify the green mechanism since steady-state creep was never attained, which may mean that more than one process is active, and the creep rates were measured over a temperature range, 300°K, which is too narrow for unambiguous interpretation of the data.⁹

In the process of plasma spraying, the ceramic powder is melted and projected onto the substrate. There is little agglomeration of the molten droplets during spraying so that the particle size of the ceramic powder determines, to a great extent, the particle size of the coating.

To determine the effect of different particle sizes, specimens were prepared from two 20% yttria-80% zirconia powders--one at Union Carbide (UC) from the Cerac powder which had particles less than 44 microns (Fig. 2), and the other at IIT Research Institute (IITRI) from Metco powder which had particles between 10 and 88 microns (Fig. 3). The results of creep testing these specimens at 1250°C and initial stresses of either 1000 or 2000 psi are shown in Fig. 17. For both stresses, the specimens prepared from the Metco powder with the larger particle size had less creep deformation than the Cerac powder with

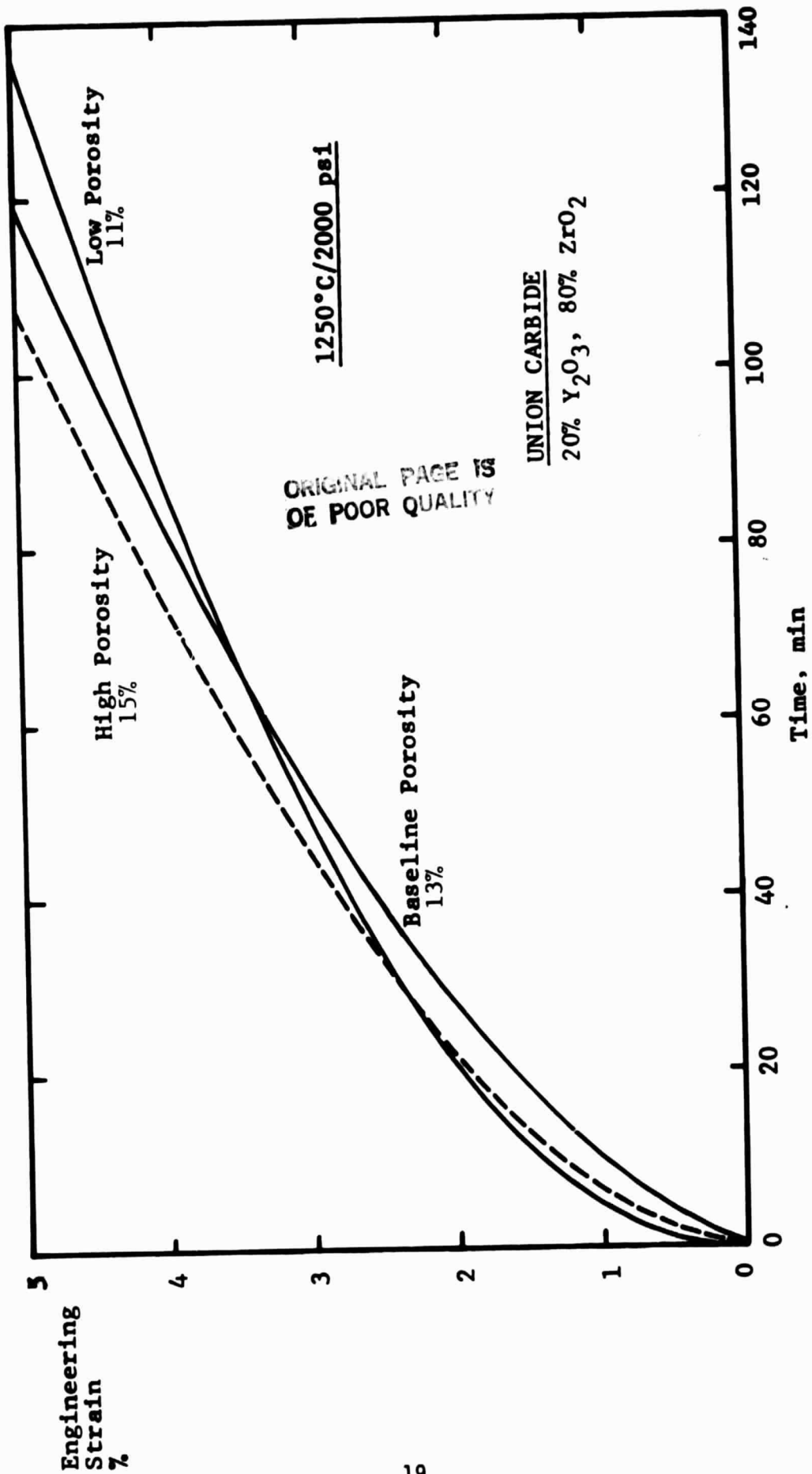


Figure 14. Typical creep curves.

Log
Engineering
Strain
% .

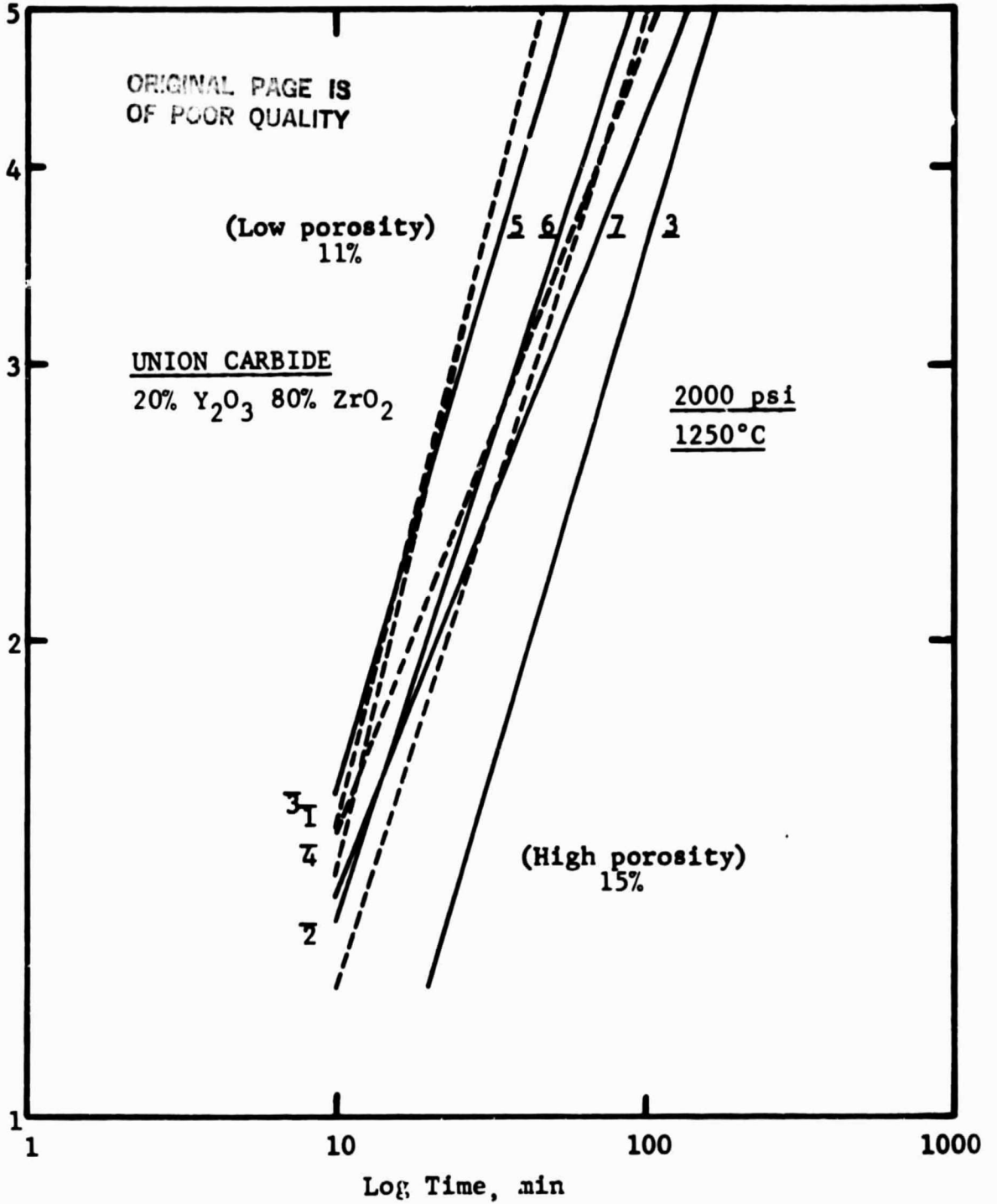


Figure 15. Effect of porosity on creep deformation.

ORIGINAL PAGE IS
OF POOR QUALITY

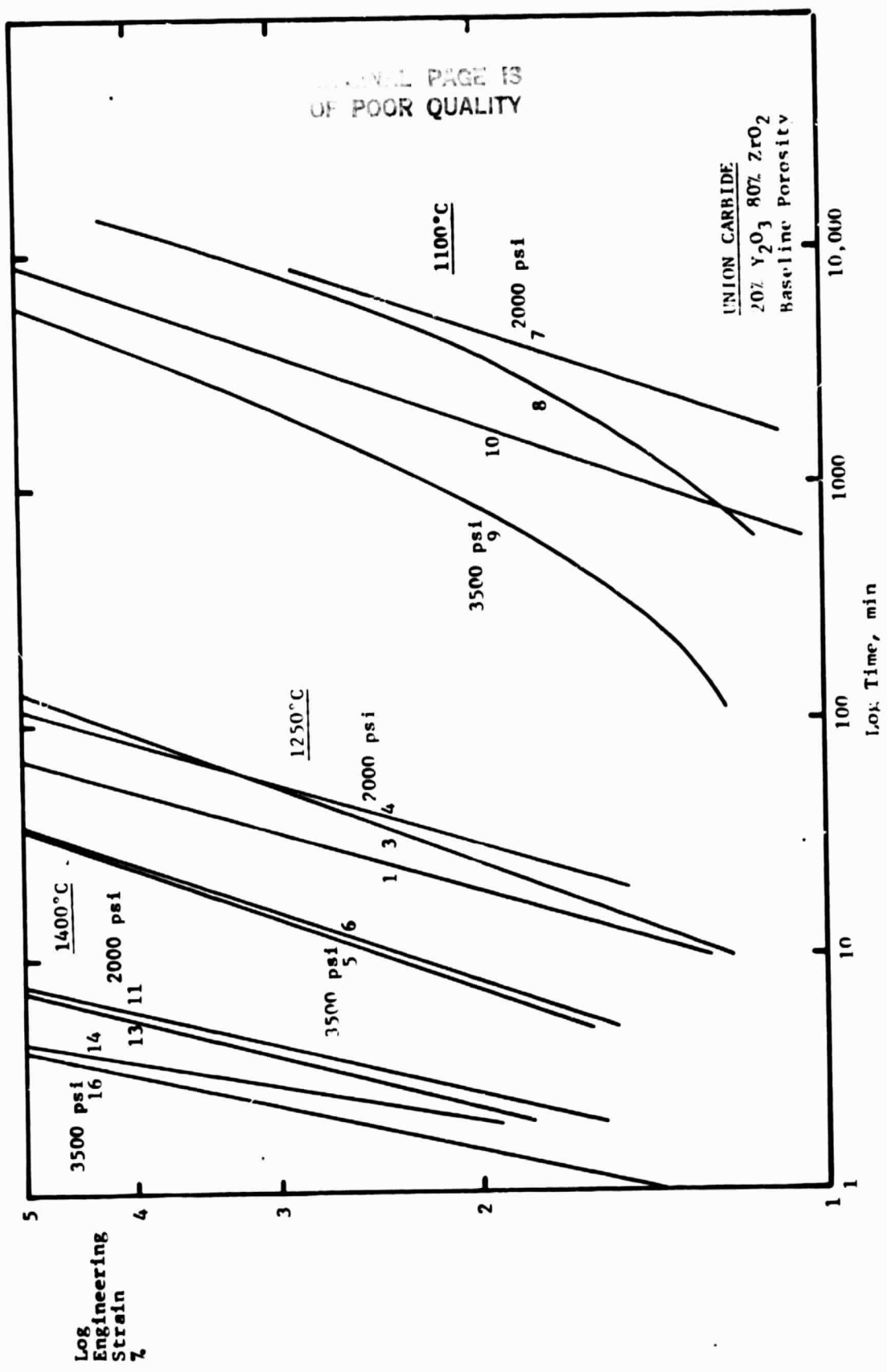


Figure 16. Effect of temperature and stress on creep deformation.

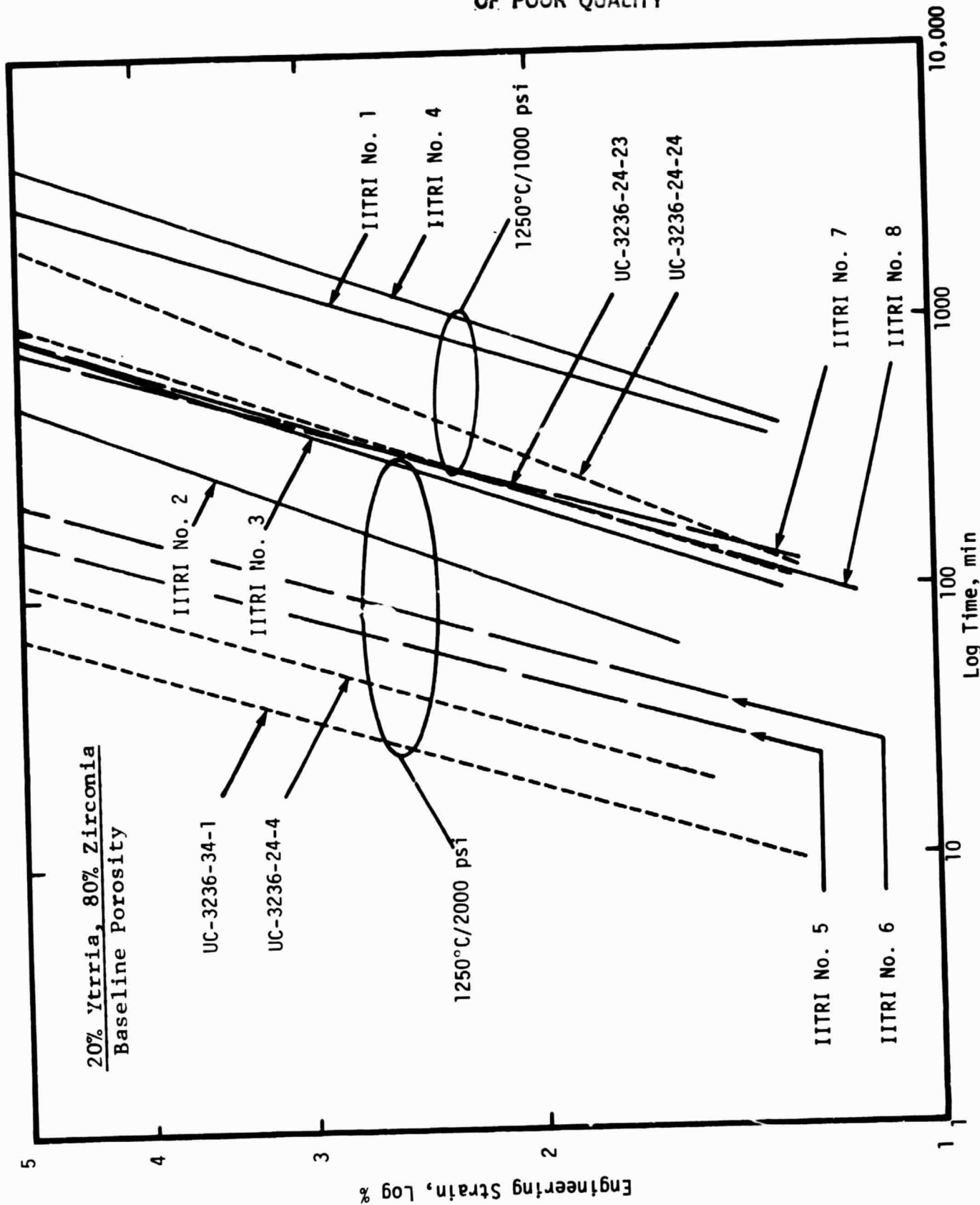


Figure 17. Effect of particle size on creep deformation.

the smaller particle size. This is the normal behavior of ceramics where creep is inversely related to grain size.

The effect of the amount of stabilization on creep was investigated by preparing specimens at IITRI from Cerac 8% yttria-92% zirconia powder with particles between 44 and 74 microns (Fig. 4) and deforming them at 1250°C and 2000 psi. The creep deformation (Fig. 18) of these specimens was intermediate between the two previous specimens and shows that increased yttria content decreases the creep rate.

The effect of different stabilizers was investigated by preparing specimens at IITRI from powders with 31% lime-69% zirconia (Fig. 5), and 21% magnesia-79% zirconia (Fig. 6). These were tested at 1250°C and 2000 psi (Fig. 19). The most rapid creep was in magnesia-stabilized specimens, lime-stabilized specimens were next, and the slowest was in the yttria-stabilized.

The difference in creep rates may be related to the phase relations in the three systems. The cubic solid solution in the yttria-zirconia system has the greatest stability and the very high liquidus temperature, T_m , of 2800°C indicates a lower overall self-diffusion rate at the creep testing temperature of 1250°C which is only 0.5 T_m (Fig. 7). The solid solution in the lime-zirconia system is stable down to at least 1400°C, but the liquidus is lower (2500°C) so that the creep temperature is 0.55 T_m and somewhat greater diffusion can occur (Fig. 8). The magnesia-zirconia system is the least stable. The cubic solid solution is stable down to only 1800°C where there is a partial transformation to a tetragonal solid solution, at 1400°C the cubic solid solution disappears and finally at 1240°C, which is very near the creep test temperature of 1250°C, monoclinic zirconia and magnesite are the stable phases (Fig. 9). The liquidus in this system is approximately 2500°C also which indicates diffusion at the creep temperature somewhat more rapid. These phase changes and different liquidus temperatures may explain the more rapid creep of magnesia-stabilized zirconia compared to lime or yttria stabilized.

The microstructure of plasma-sprayed coatings is complex. They are highly anisotropic materials composed of cracks and pores between tabular grains which form when the molten droplets hit the substrate and flatten, like snowballs thrown against a wall. A typical cross-section of part of the wall of a specimen is shown in Fig. 20. The top of the figure is the outside of

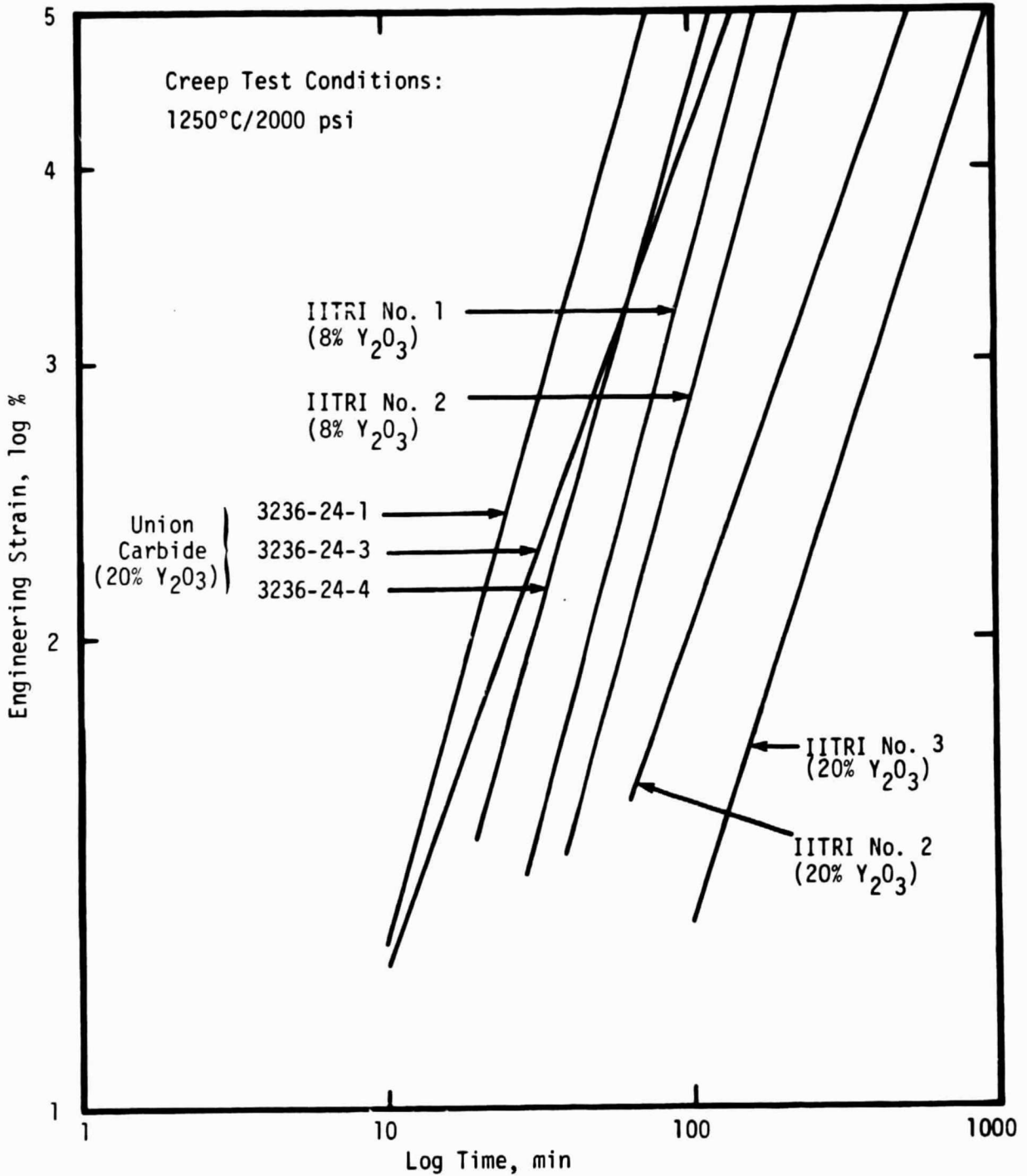


Figure 18. Effect of varying yttria content on creep deformation.

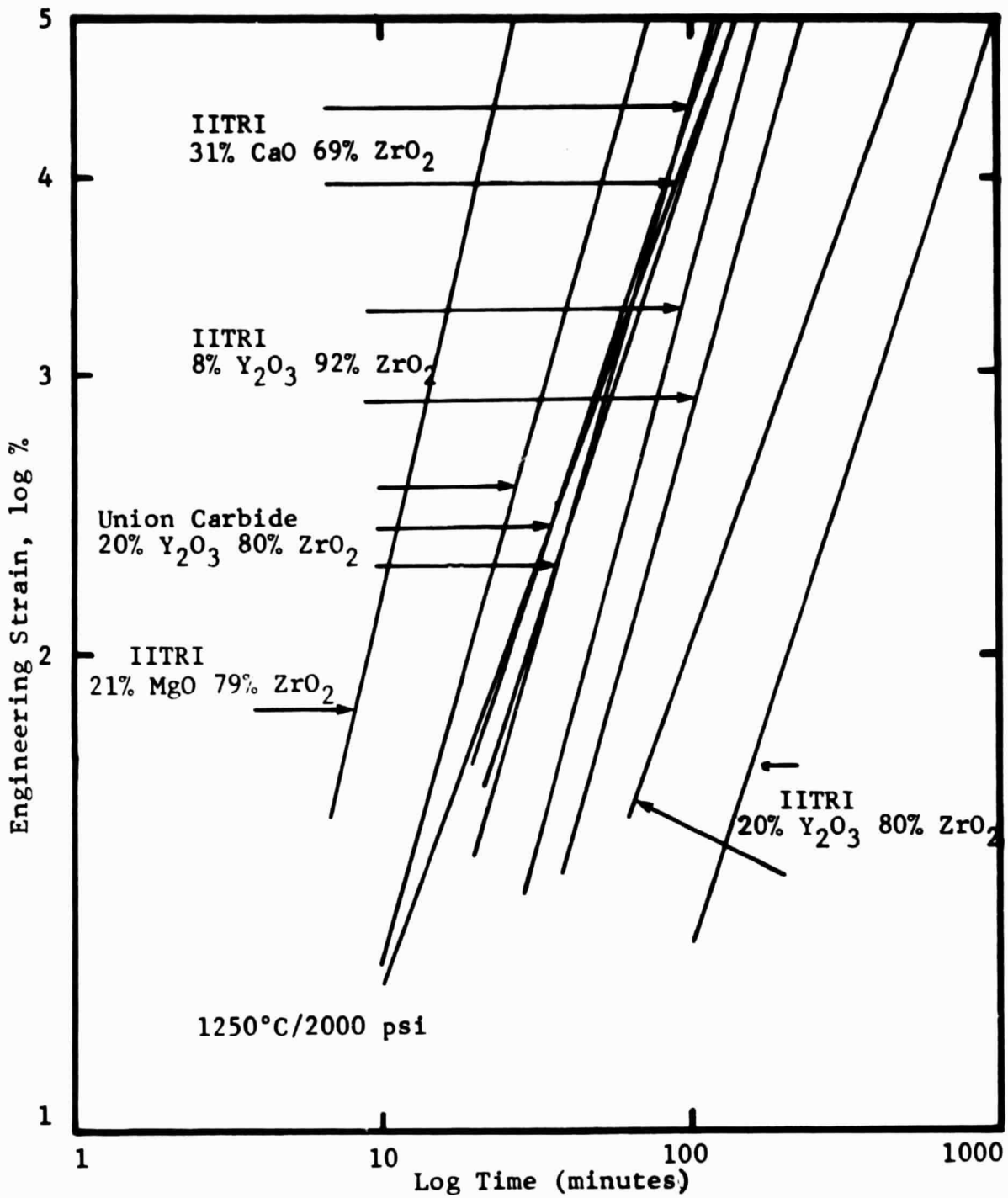
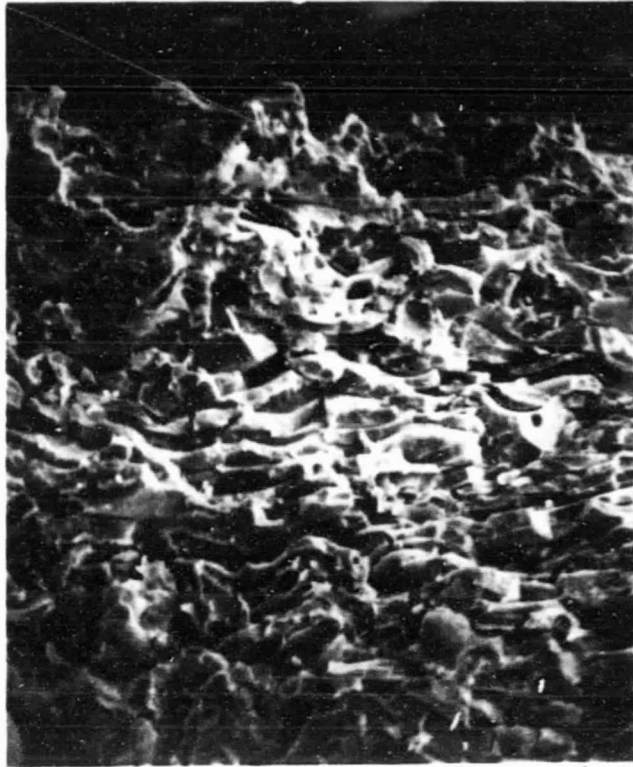


Figure 19. Effect of different stabilizers on creep deformation.



410X

Figure 20. Cross section of specimen wall showing layered particles.



410X

Figure 21. Outer surface of magnesia-stabilized zirconia uncrept specimen.

the specimen. The flattened grains are clearly shown, as are the two kinds of cracks between the grains--radial and circumferential. The radial cracks usually extend for only the thickness of one grain, but the circumferential cracks can extend for the length of several grains. A view of the outer surface which is perpendicular to the previous figure is shown in Fig. 21. The spatter fringes on the grains are shown and also cracks between the grains.

The above microstructures were typical of all untested specimens. When the tested specimens were examined, there was very little change in the appearance of the cross-section or the interior surface, but the exterior surface showed a network of polygonal cracks (Fig. 22). This was due only to creep and not to thermal shock, phase transformations, or other causes since the unloaded specimens which were adjacent to the loaded specimens during the test showed no cracking.

To summarize these observations: The specimens deformed by barreling; there was an increase in cracks on the exterior (the tensile surface), no increase on the interior (the compressive surface), and no change in porosity. It is likely that creep deformation occurred by sliding of the flat particles over each other on the exterior which produced cracking and an increase in porosity while there was a compensating decrease in porosity caused by particles sliding together on the interior surface.

ORIGINAL PAGE IS
OF POOR QUALITY



410X

Figure 22. Outer surface of magnesia-stabilized zirconia specimen after 5% creep deformation.

3. CONCLUSION

Two parameters had a pronounced effect on the creep rate of plasma-sprayed zirconia coatings: temperature and stabilization. The size of the particles sprayed and the initial stress had a lesser effect while the effect of porosity was the least. In the YSZ system, the creep rate for the 20% Y_2O_3 -80% ZrO_2 material was 1/2 to 1/3 that of the 8% Y_2O_3 -92% ZrO_2 material. Both the magnesia stabilized and calcia-stabilized materials crept at a rate 5 to 10 times that of the 20% Y_2O_3 -80% ZrO_2 material. It was directly related to temperature and porosity. Creep deformation appeared to be accommodated by cracking and particle sliding.

REFERENCES

1. R. L. Coble and W. D. Kingery, "Effect of Porosity on Physical Properties of Sintered Alumina," *J. of Amer. Ceram. Soc.*, Vol. 39, No. 11, pp. 377-385 (1956).
2. P. E. Evans, "Creep in Yttria- and Scandia-Stabilized Zirconia," *J. Amer. Ceram. Soc.*, Vol. 53, No. 7, pp. 365-369 (1970).
3. L. L. Fehrenbacher, F. P. Bailey, and N. A. McKinnon, "Compressive Creep of Yttria Rare Earth Stabilized Zirconia Storage Heater Refractories," *SAMPLE Quart.*, Vol. 2, No. 2, pp. 18-30 (1971).
4. M. S. Seltzer and P. K. Talty, "High-Temperature Creep of Y_2O_3 -Stabilized ZrO_2 ," *J. Amer. Ceram. Soc.*, Vol. 58, Nos. 3-4, pp. 124-130 (1975a).
5. M. S. Seltzer and P. K. Talty, "Creep of Low Density Yttria/Rare Earth Stabilized Zirconia," in *Deformation of Ceramic Materials*, R. D. Bradt and R. E. Tressler, eds., Plenum Press, pp. 298-312 (1975).
6. Scott, H. G., "Phase Relationships in the Zirconia-Yttria System", *J. Mater. Sci.* 10 [9] 1527-1535 (1975).
7. T. Noguchi, M. Mizuno, and W. M. Conn., *Sol. Energy*, 11 (3-4), 151 (1967).
8. C. F. Grain, "Phase Relations in the ZrO_2 -MgO System", *J. Amer. Ceram. Soc.*, 50 (6), 289 (1967).
9. Gifkins, R. C., "Transitions in Creep Behavior," *J. Mater. Sci.* 5 156-165 (1970).

APPENDIX

SPECIMEN PREPARATION INFORMATION

IIT RESEARCH INSTITUTE

ORIGINAL PAGE IS
OF POOR QUALITY

TECHNICAL NOTE NO. 78-52
MATERIALS DEVELOPMENT-TECHNOLOGY
COATINGS SERVICE DEPARTMENT, LINDE DIVISION
INDIANAPOLIS, INDIANA

DISTRIBUTION:

C. Bortz, IITRI
R. Firestone, IITRI
L. Ludwig, NASA, Lewis
D. Weisander-R. Bill, NASA, Lewis

JEJ
RWK-RJB-EGC-WGD
CBR-RHR-NLR-JFP
RCT

Author
Materials Dev. File
Library (orig. + 3)

T.A. Taylor
(AUTHOR)

June 27, 1978
(DATE)

SUBJECT Free-Standing $ZrO_2-20Y_2O_3$ Plasma Sprayed Cylinders for
IITRI Creep Measurements.



Introduction

Plasma sprayed stabilized zirconia is generally used as the outer layer of most multilayered thermal barrier systems. In one case, a thick system of the order of 90 - 170 mils, is being considered as a thermal barrier and air path seal for the first stage blade shrouds in advanced gas turbine engines. A thermal barrier coating, such as on superalloy shroud substrates, is under a complex and changing state of stress due to coating, possible heat treatment and thermal cycling in testing or in the engine. To help reduce the formation of crack-propagating tensile stresses in the outer oxide layer, heat treatment cycles have been envisioned to leave the oxide in residual compressive stress. The question then arose as to the relaxation of this stress by creep during high temperature exposure. In order to answer this question, NASA has funded IITRI to obtain creep data from three different density levels of plasma sprayed ZrO_2 - 20 wt. percent Y_2O_3 . IITRI has subcontracted the specimen preparation to Linde Coatings Service, and their preparation is described here.

ZrO₂ Powder

Twenty-five pounds of ZrO_2 stabilized with 20 wt. percent Y_2O_3 powder was obtained from Cerac, lot number 735R-A-3-A. The particle size distribution of the material produced was run by Cerac and is shown in Figure 1. We performed a second size analysis by the Rotap method (ASTM B-214) with the following results.

<u>Screen Size</u>	<u>Wt. Percent</u>
+ 200 mesh	1.99
+ 230	1.30
+ 270	4.56
+ 325	5.34
- 325	86.72
lost in testing	.09

We security screened the powder to be used for the coatings by removing any +270 mesh material. A Coulter particle size analysis was then run, showing the following size distribution. About 3 percent +270 material was removed. The discrepancies between the sieve and Coulter analyses are not unusual.



<u>Particle Diameter (microns)</u>	<u>Weight Percent After Screening</u>
+64.0	0
50.8 - 64	3.2
40.3 - 50.8	17.0
32.0 - 40.3	21.8
25.4 - 32.0	23.9
20.2 - 25.4	17.0
16.0 - 20.2	10.2
12.7 - 16.0	4.6
10.08 -12.7	1.8
8.00 -10.08	0.5
6.35 - 8.00	0.0
5.04 - 6.35	0.0
4.00 - 5.04	0.0
3.17 - 4.00	0.0
2.52 - 3.17	0.0
2.00 - 2.52	<u>0.0</u>
	100.0

Cerac ran an X-ray powder diffraction film, finding only a ZrO₂ type phase, of cubic structure and 5.13Å lattice parameter. In addition, they provided the following spectrographic analysis.

Wt. Percent, all Maximum

Ag	0.0005 - 0.005	Al	0.005 - 0.05
Ca	0.005 - 0.05	Co	0.005 - 0.05
Cr	0.0005 - 0.005	Cu	0.0005- 0.005
Fe	0.005 - 0.05	Mg	0.005 - 0.05
Mn	0.0005 - 0.005	Ni	0.01
Si	0.005 - 0.05	Sn	0.003
Ti	0.0005 - 0.005	V	0.0005- 0.005
Hf	0.1 (estimate)		



We also did X-ray diffraction on this powder. Using a bulk powder sample pressed into a specimen holder, the diffraction peaks were found on a Philips goniometer with a graphite monochromator, using copper radiation. Only a cubic phase was found with the first few diffraction lines as indicated below.

<u>(hkl)</u>	<u>d, Å</u>	<u>a₀, Å</u>
111	2.9867	5.173
200	2.5815	5.163
220	1.8250	5.162
311	1.5515	5.146

Theoretical Density

The theoretical density of ZrO₂ - 20 wt. percent Y₂O₃ was required in this program since the coatings densities were desired in three ranges of percent of theoretical:

<u>Creep Sample</u>	<u>%TD Desired</u>
High density	93 ± 3
Baseline density	85 ± 2
Low density	77 ± 3

One determination was made on the powder using a nitrogen gas null pycnometer to measure the volume occupied by a known mass of powder. This result gave a theoretical density of 6.00 gm/cm³.

Another approach is to use the X-ray diffraction data described earlier. Only a single cubic phase was observed for this material, of the same structure as pure cubic ZrO₂. From the Powder Diffraction File, 27-997 for cubic ZrO₂ we have the following.

ZrO₂, cubic

<u>(hkl)</u>	<u>d, Å</u>	<u>a₀, Å</u>
111	2.93	5.075
200	2.55	5.100
220	1.801	5.094
311	1.534	5.088

Density = 6.2 gm/cc
[Z] = 4



The molecules per unit cell, 4, arises from ZrO_2 groupings at the cube corners and cube faces of a FCC type structure. The mass of a ZrO_2 molecule is

$$\frac{123.22}{6.023 \times 10^{23}} \text{ grams}$$

Using the lattice parameter of the unit cell determined by X-ray diffraction,

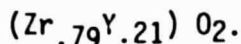
$$\text{Density} = \frac{\text{mass}}{\text{volume}} = \frac{(4)(123.22/6.023 \times 10^{23})}{(5.09 \times 10^{-8})^3} = 6.206 \text{ gm/cm}^3$$

The same can be done using the X-ray data obtained for ZrO_2 - 20 wt. percent Y_2O_3 if the average molecular weight per unit cell is known. Indicating the present material as ZrO_2 - 20 wt. percent Y_2O_3 is clearly misleading and only can refer to the component mix before firing. No Y_2O_3 is present since it would be detectable in the X-ray patterns. Y_2O_3 is BCC with distinctly different line positions from the ZrO_2 . Furthermore, chemical analyses of this material would be for Zr or Y, not as Y_2O_3 , and should not be reported as such. Upon fusion, in the concentration range here, Y enters the cubic ZrO_2 lattice as a partial replacement for Zr.

In the powder making, 20 wt. percent Y_2O_3 was charged, bringing 15.75 wt. percent yttrium, 80 wt. percent ZrO_2 , bringing 59.22 wt. percent zirconium, with the balance after fusion being oxygen, 25.03 wt. percent. As a solid solution oxide of the MO_2 type, the distribution of M between Zr and Y is thus

$$M = .79Zr + .21 Y$$

in weight percent. The atomic weights for Zr and Y are nearly the same, so this is also the distribution in atomic percent. The present " ZrO_2 - 20 wt% Y_2O_3 " is better described as



Thus, the average molecular weight of this oxide is

$$.79 (91.22) + .21 (88.9) + 32 = 122.73$$

and the X-ray density calculation can be made as follows.



$$\text{Density} = \frac{(4)(122.73/6.023 \times 10^{23})}{(5.15 \times 10^{-8})^3} = 5.97 \text{ gm/cm}^3$$

If the lattice parameter is taken instead as 5.14Å, the result is 6.00 gm/cm³.

On the basis of the two independent measurements described, we will use 6.00 gm/cm³ as the theoretical density of the present powder.

Coating Preparation

Aluminum tubing was cut to length and turned straight and true to 0.25 inch diameter. These were lightly grit blasted for adherence during coating and subsequent machining operations.

Plasma Spraying

A number of aluminum tubes were coated under identical plasma torch conditions for each density range. As agreed upon, AMS 2437 plasma spray control sheets were filled out for each coating type, and are included in the Appendix. It is clear, however, that the gas flows and torch parameters are only applicable to a Linde plasma spraying system.

Preparation of Free-Standing Cylinders

The coated aluminum tubes were parted through at 0.50 inch lengths using a tool post grinder with a diamond cutting wheel, as the tubes were turning on a lathe. The individual tubes were then held in a special made nylon collet and internally bored to remove all but about 5 mils of aluminum from the tube wall.

The residual aluminum was leached out in 15% NaOH at 60°C and cleaned as follows.

<u>Operation</u>		<u>Minutes</u>
Leaching	15% NaOH, 60°C	13 - 18
Rinsing	distilled water, 95°C	1
Rinse	distilled water, 25°C	1
Clean	distilled water, 25°C, ultrasonic	3
Clean	Methanol, 25°C, ultrasonic	3
Dry	Air, 25°C	5 - 10
Vacuum dry	vacuum oven, -30 inch Hg, 92°C	120



The final product, 0.50 inch long cylinders, 0.25 inch ID, .030 inch wall thickness, were individually inspected at 10X magnification, then each packed separately in protective polyviols. The number shipped were

high density	14 pieces
base line density	32 pieces
low density	14 pieces

Six baseline samples were shipped early to aid the IITRI test schedule. The remaining samples were divided into two lots, each containing half of each density type, and shipped separately on two succeeding days.

Coating Density

Identically produced free-standing oxide cylinders were measured for apparent density by ASTM B 328-60. Leached at the same time as the IITRI samples, these 0.50 inch long tubes were slit longitudinally into two halves with a diamond saw. This was done to allow blotting of excess oil from the inside of the tube, as per the ASTM method. The final absolute density value was corrected for the density of the water bath used for immersion at its temperature during the measurement period. Finally, the percent of theoretical density was calculated for the average of four determinations on nominal 0.5 gram samples.

<u>Density Type</u>	<u>High</u>	<u>Baseline</u>	<u>Low</u>
Individual	5.302	5.217	5.081
Densities,	5.318	5.205	5.084
gm/cm ³	5.347	5.220	5.084
	5.318	5.210	5.081
Average density	5.321	5.213	5.082
Standard deviation	0.0188	0.0068	0.0017
Percent of theoretical,	88.69	86.89	84.71
6.00 gm/cm ³			

Compared to the desired density ranges for this program, the baseline density was achieved, and the high density was short by 1.3 percent. The low density of 74-80 could not be obtained, as pointed out to IITRI and NASA at the start of the program. However, the value obtained of 84.7 percent of theoretical does produce a substantially different structure and has substantially different mechanical strength than the baseline or high density samples.



It was agreed upon earlier that devices to extend the density range, such as heat treatment or fugitive agents would not be used.

Coating Microstructures

Identically produced free-standing oxide tubes were cut longitudinally and then freshly fractured longitudinally again, just prior to observation by scanning electron microscopy. The micrographs for each of the high, baseline, and low density samples are shown in Figures 2 through 4. In all micrographs the coating direction is across the short dimension of the picture.

It is seen that the density variation arises due to the controlled amount of inter-splat separation or porosity. The splat particles themselves are fully dense. It is also likely that mechanical properties will be anisotropic in the two lower density samples, as the pancake splat structure is quite evident. In the analysis of longitudinal compressive deformation, the mechanism of splat boundary sliding should not be overlooked. It is clear that the splats themselves have a finer grain structure within but of much higher cohesive nature than the intersplat boundaries.

Acknowledgments

The coating work on this program was ably carried out by Roy Newman. Careful density measurements were made by Bob O'Connell. The consultations on torch parameters for special density effects with Merle Weatherly was greatly appreciated.

References

"Creep Evaluation of Plasma Sprayed ZrO₂ Materials",
NASA RFP 3-835240Q
NASA Contract NAS 3-20828
IITRI Project No. D6147

UCC Databooks

3236-13 to 29 (coating)
3274-2 (density)
3281-75 (X-ray)

UCC Powder Analyses 6475, 6516

IITRI P.O. 65133
UCC Invoice L-27132

UCC Specimen No.

high density 3236-29-1 thru 14
baseline density 3236-24-1 thru 32
low density 3236-28-1 thru 14


T.A. Taylor

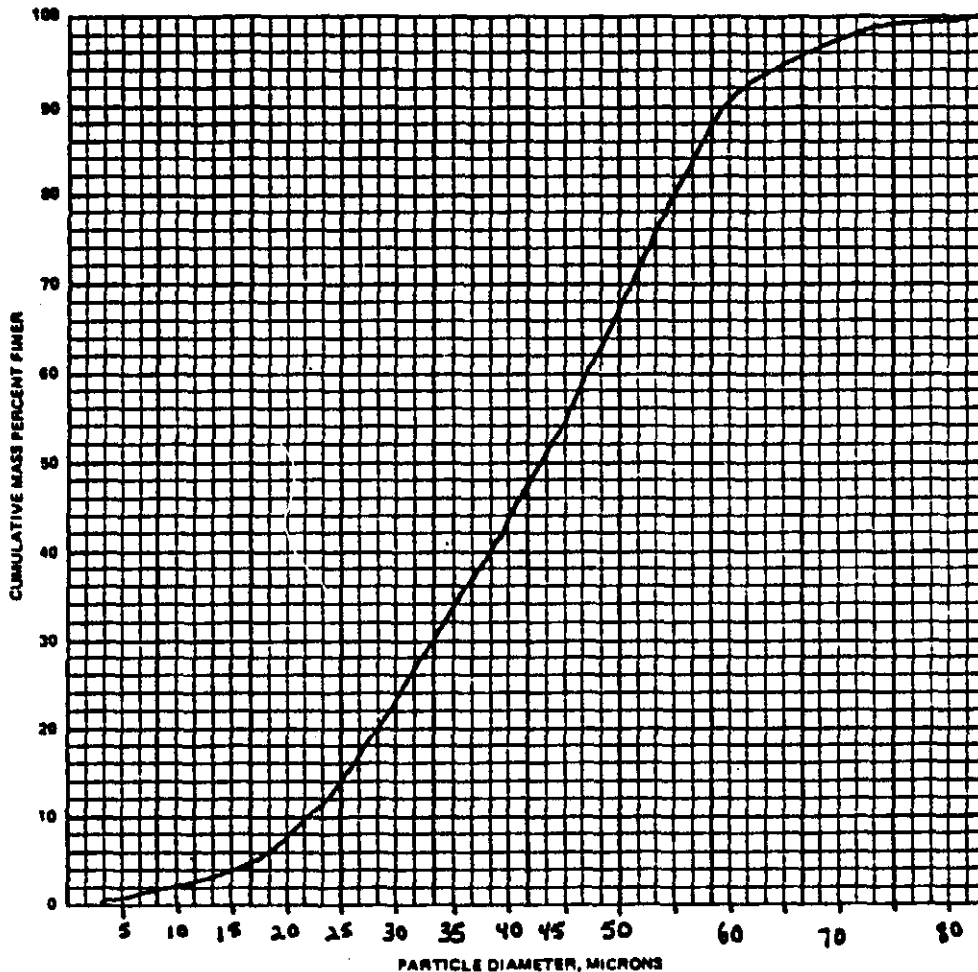




PARTICLE SIZE DISTRIBUTION REPORT

MATERIAL: ZrO₂ - Y₂O₃ DATE: 3-29-78
CUSTOMER NAME: _____ CUSTOMER LOT NO.: _____
CERAC STOCK NO.: Z- CERAC LOT NO.: 735B-A-3-A
RUN NO.: 1 OPERATOR: Tom S. REQUESTED BY: Paul J.
COMMENTS (if any): ETHYLENE GLYCOL was used for dispersion

PLEASE NOTE: Particle size above 44 microns are done by screening. Ignore this portion of curve as it is not necessarily consistent with screen results.



EQUIVALENT SPHERICAL DIAMETER (from 50% point): 42.8 MICRONS MEASURED FISHER SUB-SIEVE SIZE: >25 MICRONS

Figure 1. Powder size distribution of Cerac ZrO₂ - 20 wt. percent Y₂O₃.



ORIGINAL PAGE IS
OF POOR QUALITY

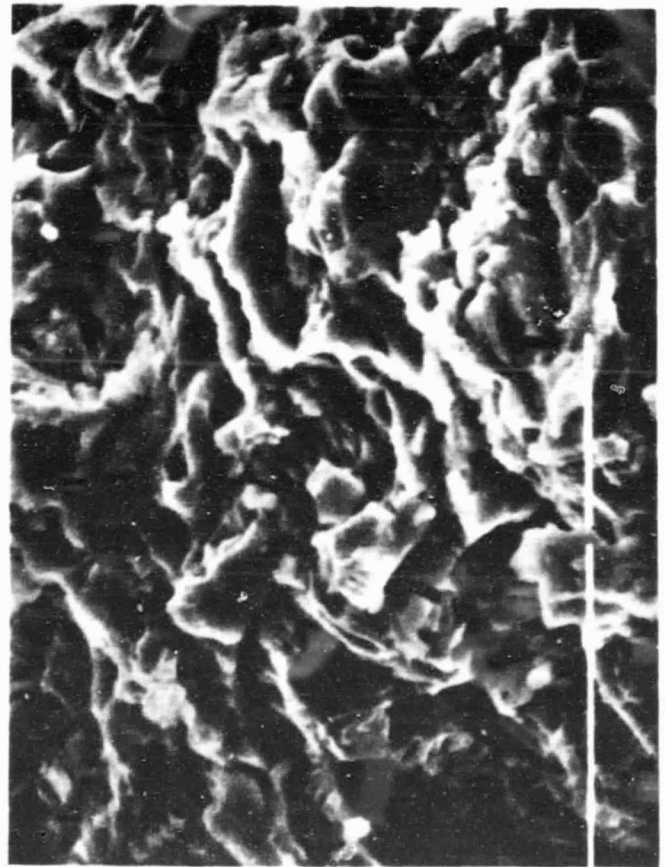
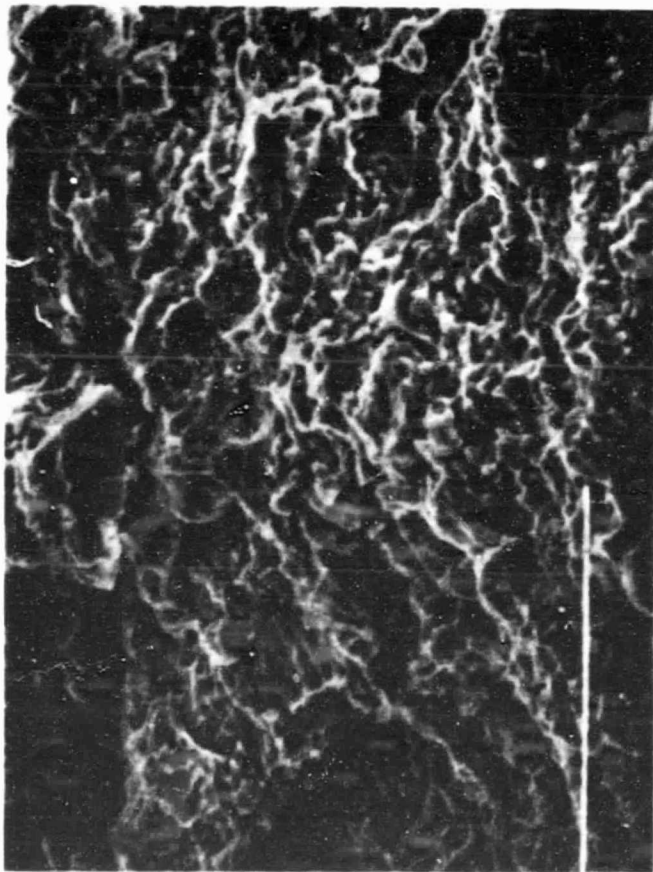
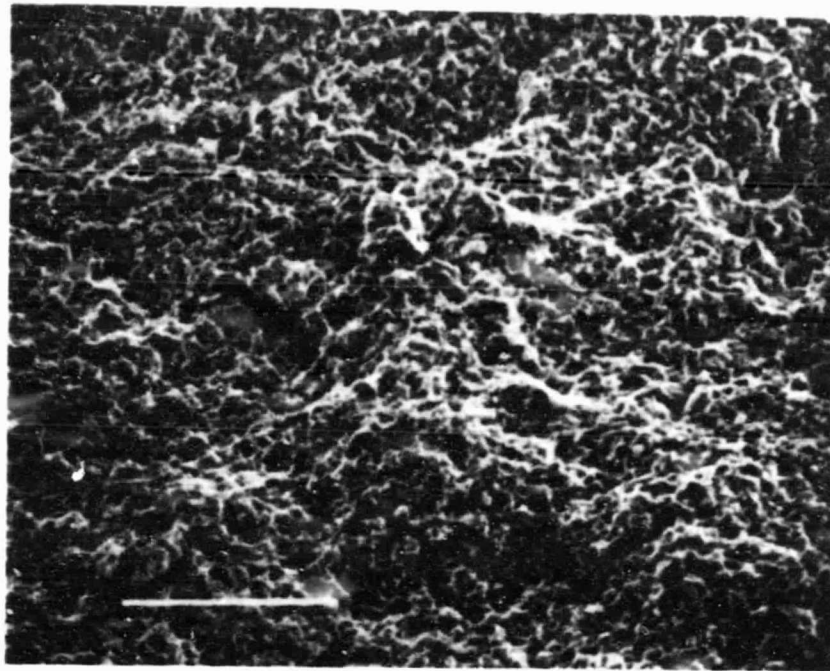


Figure 2. SEM micrographs, high density ZrO_2 sample in fractured cross-section. 391, 1170 and 3900X magnifications. 6.4 micron bar (separated stripe) is shown at the high magnification.



ORIGINAL PAGE IS
OF POOR QUALITY

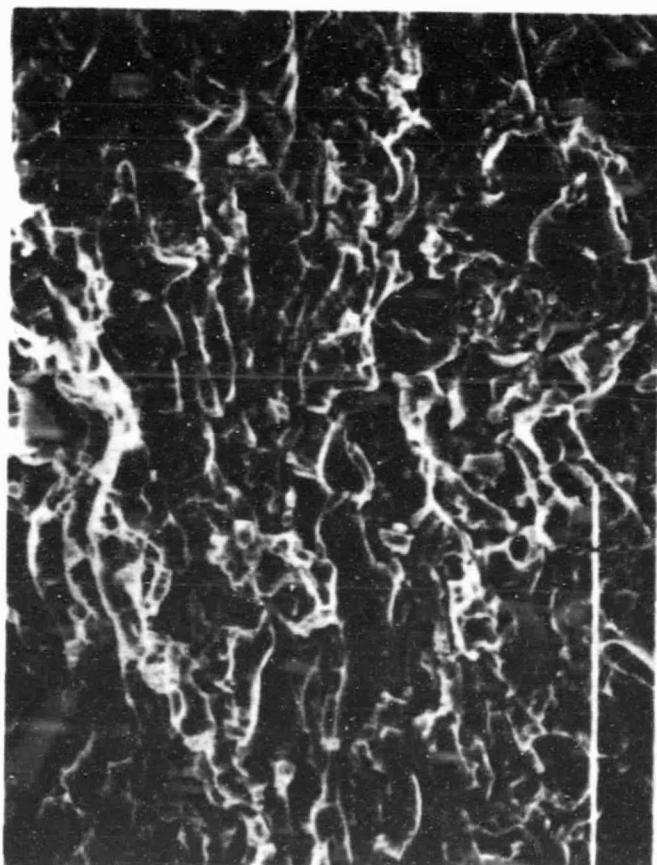
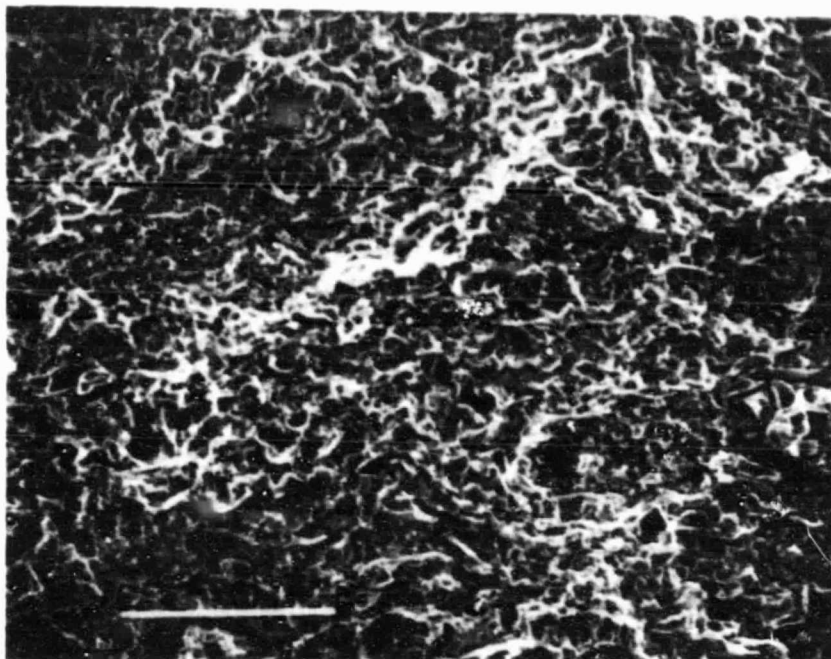


Figure 3. SEM micrographs, baseline density ZrO_2 sample in fractured cross-section. 390, 1170 and 3900X magnifications. 6.4 micron bar (separated stripe) is shown at the high magnification.



ORIGINAL PAGE IS
OF POOR QUALITY

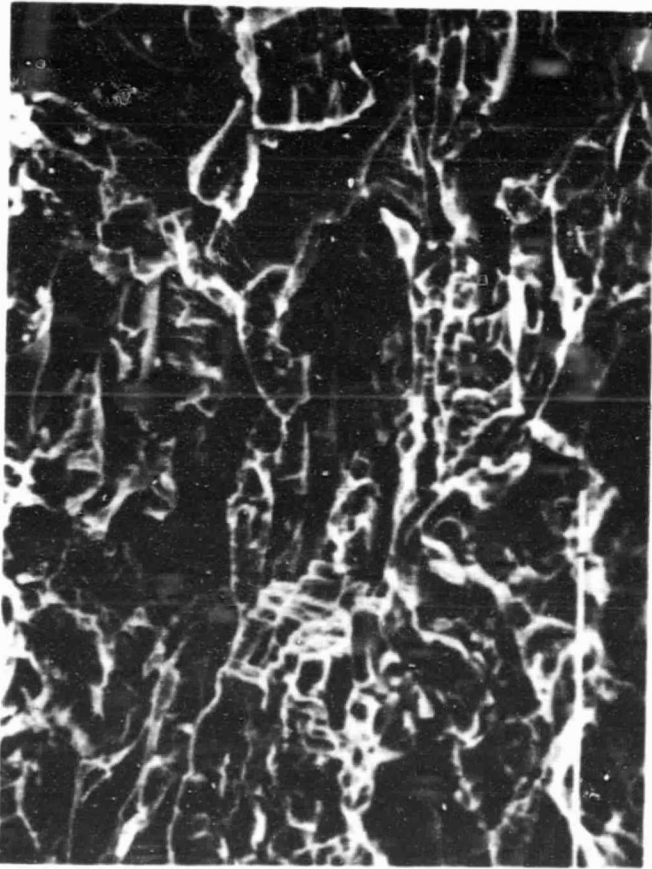
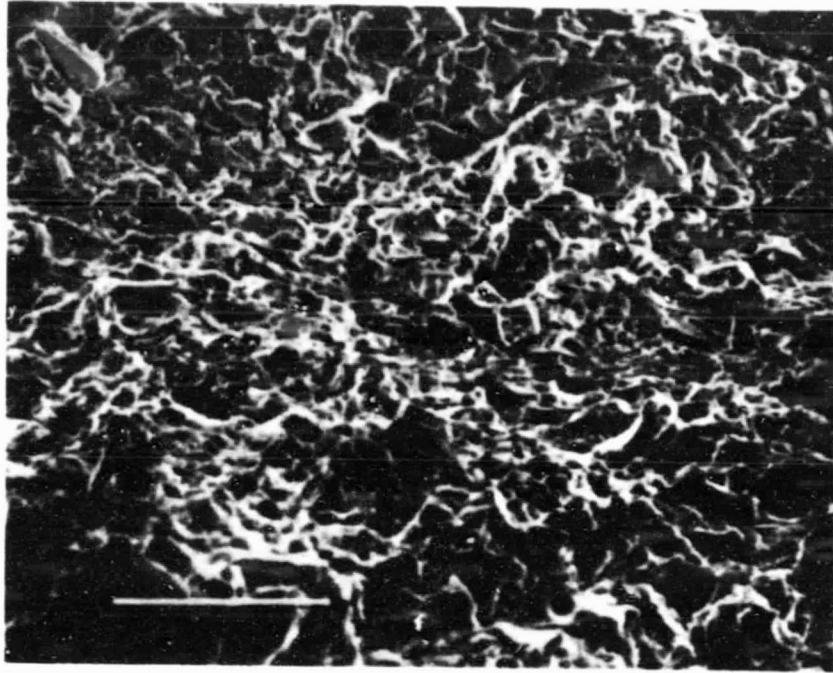


Figure 4. SEM micrographs, low density ZrO_2 sample in fractured cross-section. 390, 1170 and 3900X magnifications. 6.4 micron bar (separated stripe) is shown at the high magnification.



Appendix

**AMS 2437
Plasma Spray Control Sheets**



PLASMA SPRAY CONTROL SHEET

PART NAME Low Density PLASMA SPRAY COMPANY NAME LINDE
 PART NO. Creep Sample Coatings Service
 AREA TO BE COATED 1/4" d x 2" Aluminum tube

PREPARATION

Pre Blast Cleaning Acetone, Alcohol
 Blast Masking Fixture No. N/A
 Blasting Grit: Type Al₂O₃ Size 54 Air Pressure, psi 10

EQUIPMENT

Manufacture Type LINDE Plasma System No. 1108-D
 Gun Nozzle Proprietary Electrode Proprietary Powder Port Proprietary
 Spraying Mask Fixture No. N/A
 Special Adapters N/A

CONSOLE

Primary Gas Nitrogen Console, psi 31 Flow, CFH 40
 Secondary Gas Hydrogen Console, psi 72 Flow, CFH 20
 Amperage, D.C., Operating 100
 Voltage D.C., Operating 105 Voltage D.C., Open Circuit N/A
 Power Control Kilowatt Level: Start N/A Finish _____
 Primary Gas Dew Point N/A Secondary Gas Dew Point _____

POWDER FEEDER

Carrier Gas Nitrogen Flow, CFH 40
 Powder Feed Mechanism N/A Powder Feed, RPM N/A
 Vibrator: On N/A Off N/A Feeder Hose: Diameter N/A Length N/A
 Vibration Amplitude N/A

COATING MATERIAL

Material Identification ZrO₂ - 20 wt% Y₂O₃ lot 7358-A-3-A
 Spray Rate 60 gm/min. Spray Distance 0.75"

COATING DATA

Required Coating Thickness .030" After Spraying _____
 Part Dimension: Before Spraying _____
 Pre Heat Temp N/A Maximum Part Temp N/A
 Spray Time (Per Cycle) N/A Cool Time (Per Cycle) N/A
 Method of Cooling N/A
 Position of Cooling N/A

WORK HANDLING EQUIPMENT

Part Proprietary Gun _____
 Part Speed _____ Gun Speed _____

QUALITY CONTROL

Cup & Bend Panel See report text. Metallography _____
 Bond Specimen _____

OPERATOR _____ CERTIFICATION NO. _____

APPROVAL _____



PLASMA SPRAY CONTROL SHEET

PART NAME High Density PLASMA SPRAY COMPANY NAME LINDE
PART NO. Creep Sample Coatings Service
AREA TO BE COATED 1/4" d x 2" Aluminum Tube

PREPARATION

Pre Blast Cleaning Acetone, Alcohol
Blast Masking Fixture No. N/A
Blasting Grit: Type Al₂O₃ Size 54 Air Pressure, psi 10

EQUIPMENT

Manufacture Type LINDE Plasma System No. 1108-A
Gun Nozzle Proprietary Electrode Proprietary Powder Port Proprietary
Spraying Mask Fixture No. N/A
Special Adapters N/A

CONSOLE

Primary Gas Argon Console, psi 250 Flow, CFH 190
Secondary Gas Hydrogen Console, psi 75 Flow, CFH 20
Amperage, D. C., Operating 150
Voltage D. C., Operating 80 Voltage D. C., Open Circuit N/A
Power Control Kilowatt Level: Start N/A Finish N/A
Primary Gas Dew Point N/A Secondary Gas Dew Point N/A

POWDER FEEDER

Carrier Gas Argon Flow, CFH 100
Powder Feed Mechanism N/A Powder Feed, RPM N/A
Vibrator: On N/A Off N/A Feeder Hose: Diameter N/A Length N/A
Vibration Amplitude N/A

COATING MATERIAL

Material Identification ZrO₂ - 20 wt% Y₂O₃ lot 7358-A-3-A
Spray Rate 30 gm/min. Spray Distance 0.50"

COATING DATA

Required Coating Thickness .030" After Spraying N/A
Part Dimension: Before Spraying N/A
Pre Heat Temp N/A Maximum Part Temp N/A
Spray Time (Per Cycle) N/A Cool Time (Per Cycle) N/A
Method of Cooling N/A
Position of Cooling N/A

WORK HANDLING EQUIPMENT

Part Proprietary Gun N/A
Part Speed N/A Gun Speed N/A

QUALITY CONTROL

Cup & Bend Panel See report text. Metallography N/A
Bond Specimen N/A

OPERATOR N/A CERTIFICATION NO. N/A

APPROVAL N/A



PLASMA SPRAY CONTROL SHEET

PART NAME Normal Density PLASMA SPRAY COMPANY NAME LINDE
 PART NO. Creep Sample Coatings Service
 AREA TO BE COATED 1/4" d x 2" Aluminum Tube

PREPARATION

Pre Blast Cleaning Acetone, Alcohol
 Blast Masking Fixture No. N/A
 Blasting Grit: Type Al₂O₃ Size 54 Air Pressure, psi 10

EQUIPMENT

Manufacture Type LINDE Plasma System No. 1108-D
 Gun Nozzle Proprietary Electrode Proprietary Powder Port Proprietary
 Spraying Mask Fixture No. N/A
 Special Adapters N/A

CONSOLE

Primary Gas Argon Console, psi 66 Flow, CFH 35
 Secondary Gas Nitrogen Console, psi 125 Flow, CFH 17
 Amperage, D. C., Operating 100
 Voltage D. C., Operating 82 Voltage D. C., Open Circuit N/A
 Power Control Kilowatt Level: Start N/A Finish _____
 Primary Gas Dew Point N/A Secondary Gas Dew Point _____

POWDER FEEDER

Carrier Gas Nitrogen Flow, CFH 60
 Powder Feed Mechanism N/A Powder Feed, RPM N/A
 Vibrator: On N/A Off N/A Feeder Hose: Diameter N/A Length N/A
 Vibration Amplitude N/A

COATING MATERIAL

Material Identification ZrO₂ - 20 wt% Y₂O₃ lot 7358-A-3-A
 Spray Rate 60 gm/min. Spray Distance 0.75"

COATING DATA

Required Coating Thickness 0.32" After Spraying _____
 Part Dimension: Before Spraying _____
 Pre Heat Temp N/A Maximum Part Temp N/A
 Spray Time (Per Cycle) N/A Cool Time (Per Cycle) N/A
 Method of Cooling N/A
 Position of Cooling N/A

WORK HANDLING EQUIPMENT

Part Proprietary Gun _____
 Part Speed _____ Gun Speed _____

QUALITY CONTROL

See report text. Metallography _____
 Cup & Bend Panel _____
 Round Specimen _____

OPERATOR _____ CERTIFICATION NO. _____

APPROVAL _____



Index

Subject - Creep Specimens
 - Thermal Barrier
Coating - ZrO₂-Y₂O₃
Customer - IITRI
 NASA, Lewis

ORIGINAL PAGE IS
OF POOR QUALITY



Sponsor NASA
Project No. M

Date 6/80 (21)
Test No. _____

PART

Substrate No. .750 Al TUBE Type _____
Fixture No. _____

ORIGINAL PAGE IS
OF POOR QUALITY

PREPARATION

Pre-blast Cleaning ACETONE
Blasting Grit: Type _____ Size S.S. WHITE
Post-blast Cleaning ACETONE
Masking TAPE

EQUIPMENT

Spray Gun SG-1B(SI-AS version) Cathode SI-3-R-05 Anode SI-3-F-05
Powder Injection INTERNAL
Fixture No. _____

CONSOLE

Arc Gas LINDE Air (P.P.) psi 50 Flow, CFH(reading) 67 (1.6)
Powder Feed Gas S.A.A. psi 30 Flow, CFH(reading) 21 (.4)
Amps. DC 500 Volts, AC 26 OCV 86 Arc Time _____

POWDER FEEDER

Hopper Type: Sylvester Vibratory Screw Feeder
Hopper No. 2 ScrewFeed RPM(Setting) 12.5 (50) Vibrator STANDARD
Amt. Powder Added To Hopper _____

COATING MATERIAL

Identification 202
Size Range _____

COATING DATA

Required Thickness .030 Thickness After Spray .008
Spray Distance _____ Spray Rate _____
No. of Passes: Horizontal 30-30-30 Vertical _____
Part Preheat Temp. MEKER Max. Part Temp. _____
Part Speed _____ Gun Speed _____ Spray Time _____

COMMENTS

LATHE

Sponsor NASA

Date 3-20-68

Project No. 10071

Test No. _____

ORIGINAL PAGE IS
OF POOR QUALITY

PART

Substrate No. 252 A1 TUBE Type _____

Fixture No. LP-1E

PREPARATION

Pre-blast Cleaning ACETONE

Blasting Grit: Type 100 Size _____

Post-blast Cleaning ACETONE

Masking _____

EQUIPMENT

Spray Gun SG-1B(S1-AS version) Cathode S1-3-R-25 Anode S1-3-F-25

Powder Injection _____

Fixture No. 4-V

CONSOLE

Arc Gas Argon (P.A.) psi 30 Flow, CFH(reading) 11

Powder Feed Gas Argon psi 30 Flow, CFH(reading) 10

Amps. DC 500 Volts, DC 26 OCV _____ Arc Time _____

POWDER FEEDER

Hopper Type: Sylvester Vibratory Screw Feeder

Hopper No. _____ ScrewFeed RPM(Setting) 50(12.5) Vibrator STANDARD

Amt. Powder Added To Hopper TO COVER

COATING MATERIAL

Identification 302 NS 2nd - 400 - STABILIZED

Size Range _____

COATING DATA

Required Thickness .004 TO .031 Thickness After Spray _____

Spray Distance 4" Spray Rate _____

No. of Passes: Horizontal 300 Vertical _____

Part Preheat Temp. _____ Max. Part Temp. _____

Part Speed _____ Gun Speed _____ Spray Time _____

COMMENTS

Sponsor NASA

Date 3/11/61

Project No. M6071

Test No. _____

PART

Substrate No. .251 Al Tub Type _____

Fixture No. LATHE

ORIGINAL PAGE IS
OF POOR QUALITY

PREPARATION

Pre-blast Cleaning ACETONE

Blasting Grit: Type 55 WHITE Size _____

Post-blast Cleaning ACETONE

Masking TAPE

EQUIPMENT

Spray Gun SG-1B(S1-AS version) Cathode S1-3-R-04 Anode S1-3-F-05

Powder Injection INTERNAL

Fixture No. _____

CONSOLE

Arc Gas Ar (AIR PRODUCTS) psi 50 Flow, CFH(reading) 1.6

Powder Feed Gas S.A.A. psi 30 Flow, CFH(reading) .4

Amps. DC 500 Volts, DC 24 OCV 84 Arc Time _____

POWDER FEEDER

Hopper Type: Sylvester Vibratory Screw Feeder

Hopper No. 2 ScrewFeed RPM(Setting) 50 (12.5) Vibrator STD.

Amt. Powder Added To Hopper _____

COATING MATERIAL

Identification 202 NS 2.02 - 4.03 STAB.

Size Range _____

COATING DATA

Required Thickness .024 TO .031 Thickness After Spray _____

Spray Distance 4.0" Spray Rate _____

No. of Passes: Horizontal 300 Vertical _____

Part Preheat Temp. TORCH Max. Part Temp. _____

Part Speed _____ Gun Speed _____ Spray Time _____

COMMENTS

Sponsor NASA
Project No. M06071

Date 6/16
Test No. _____

PART

Substrate No. .250" o.d. AI TUBE Type _____
Fixture No. _____

ORIGINAL PAGE IS
OF POOR QUALITY

PREPARATION

Pre-blast Cleaning ACETONE
Blasting Grit: Type SS WHITE Size _____
Post-blast Cleaning ACETONE
Masking TAPE

EQUIPMENT

Spray Gun SG-1B(S1-AS version) Cathode S1-3-R-05 Anode S1-3-F-05
Powder Injection INTERNAL
Fixture No. _____

CONSOLE

Arc Gas Ar (AIR PRODUCTS) psi 50 Flow, CFH(reading) 1.6
Powder Feed Gas S.A.A. psi 30 Flow, CFH(reading) .4
Amps. DC _____ Volts, DC _____ OCV 84 Arc Time _____

POWDER FEEDER

Hopper Type: Sylvester Vibratory Screw Feeder
Hopper No. 2 ScrewFeed RPM(Setting) 50 (12.5) Vibrator STD.
Amt. Powder Added To Hopper _____

COATING MATERIAL

Identification 202 NS ZnO₂ + 1/2 O₃ STAB.
Size Range _____

COATING DATA

Required Thickness .024 TO .031 Thickness After Spray .025
Spray Distance 4.0 Spray Rate _____
No. of Passes: Horizontal 300 Vertical _____
Part Preheat Temp. TOUCH Max. Part Temp. _____
Part Speed _____ Gun Speed _____ Spray Time _____

COMMENTS

Sponsor: NASA LEWIS Date _____
Project No. M06071 Test No. _____

PART

Substrate No. .251 Al TUBE Type _____
Fixture No. _____

ORIGINAL PAGE IS
OF POOR QUALITY

PREPARATION

Pre-blast Cleaning ACETONE
Blasting Grit: Type S.C Size 55 WHITE
Post-blast Cleaning ACETONE
Masking TAPE

EQUIPMENT

Spray Gun SG-1B(S1-AS version) Cathode S1-3-R-05 Anode S1-3-F-07
Powder Injection INTERNAL
Fixture No. _____

CONSOLE

Arc Gas Ar (AIR PRODUCTS) psi 50 Flow, CFH(reading) 1.6
Powder Feed Gas _____ psi 30 Flow, CFH(reading) .4
Amps. DC _____ Volts, DC _____ OCV 84 Arc Time _____

POWDER FEEDER

Hopper Type: Sylvester Vibratory Screw Feeder
Hopper No. 2 ScrewFeed RPM(Setting) 50(12.5) Vibrator STD
Amt. Powder Added To Hopper _____

COATING MATERIAL

Identification ZnO₂ + 8% Y₂O₃
Size Range -200 +325

COATING DATA

Required Thickness .024 TO .031 Thickness After Spray _____
Spray Distance 4.0 " Spray Rate _____
No. of Passes: Horizontal ~~510~~ 510 Vertical _____
Part Preheat Temp. TORCH Max. Part Temp. _____
Part Speed _____ Gun Speed _____ Spray Time _____

COMMENTS

PLASMA DATA

Sponsor NASA LEWIS Date _____

Project No. MB6071 Test No. _____

PART

ORIGINAL PAGE IS
OF POOR QUALITY

Substrate No. 0.251" AI TYPE Type _____

Fixture No. _____

PREPARATION

Pre-blast Cleaning ACETONE

Blasting Grit: Type S.C Size SS WHITE

Post-blast Cleaning ACETONE

Masking TAPE

EQUIPMENT

Spray Gun SG-1B(S1-AS version) Cathode S1-3-R-05 Anode S1-3-F-07

Powder Injection INTERNAL

Fixture No. _____

CONSOLE

Arc Gas Ar (AIR PRODUCTS) psi 50 Flow, CFH(reading) 1.6

Powder Feed Gas _____ psi 30 Flow, CFH(reading) .4

Amps. DC _____ Volts, DC _____ OCV 84 Arc Time _____

POWDER FEEDER

Hopper Type: Sylvester Vibratory Screw Feeder

Hopper No. 1 ScrewFeed RPM(Setting) 50(12.5) Vibrator STD.

Amt. Powder Added To Hopper TO COVER SCREW

COATING MATERIAL

Identification METCO #211 CALCIUM ZIRCONATE

Size Range _____

COATING DATA

Required Thickness .024 TO .031" Thickness After Spray _____

Spray Distance 4.0" Spray Rate _____

No. of Passes: Horizontal _____ Vertical _____

Part Preheat Temp. TORCH Max. Part Temp. _____

Part Speed _____ Gun Speed _____ Spray Time _____

COMMENTS

PLASMA DATA

Sponsor RSS

Date 2/25/79 (12)

Project No. _____

Test No. _____

PART

ORIGINAL PAGE IS
OF POOR QUALITY

Substrate No. _____

Type SS CYCLONE TEST SAMPLES

Fixture No. _____

PREPARATION

Pre-blast Cleaning NONE

Blasting Grit: Type ? Size TOWN STAIRS SAND BLASTER

Post-blast Cleaning ALCONOX & WARM WATER, ACETONE ETC.

Masking NONE

EQUIPMENT

Spray Gun SG-1B(S1-AS version) Cathode S1-3-R-02 Anode S1-3-F-02

Powder Injection INTERNAL

Fixture No. NONE - HAND HELD

CONSOLE

Arc Gas Ar (METHESON 99.998%) psi 50 Flow, CFH(reading) 67(1.6)

Powder Feed Gas SAME AS ABOVE psi 30 Flow, CFH(reading) 21(.4)

Amps. DC _____ Volts, DC _____ OCV 84 Arc Time _____

POWDER FEEDER

Hopper Type: Sylvester Vibratory Screw Feeder

Hopper No. 2 ScrewFeed RPM(Setting) 50(12.5) Vibrator SANCO

Amt. Powder Added To Hopper _____

COATING MATERIAL

Identification CERAC ZnO₂ (5% CaO)

Size Range -325 + 10 MICRONS

COATING DATA

Required Thickness _____ Thickness After Spray _____

Spray Distance _____ Spray Rate _____

No. of Passes: Horizontal _____ Vertical _____

Part Preheat Temp. MEKER BURNER Max. Part Temp. _____

Part Speed _____ Gun Speed 1'/SEC Spray Time _____

COMMENTS